Conflicting "Ages" of Tertiary Basalt and Contained Fossilized Wood, Crinum, Central Queensland, Australia

Andrew A. Snelling, PhD,*
Answers In Genesis, PO Box 6302, Acacia Ridge, DC, Queensland, Australia, 4110.

*current address: Answers in Genesis PO Box 510, Hebron, Kentucky, 41048, USA.

Published in: Creation Ex Nihilo Technical Journal*, volume 14, number 2, 2000, pp. 99-122.*

Abstract

Fossilized wood found entombed in a Tertiary basalt flow at Crinum in central Queensland was identified as probably *Melaleuca*, and yielded a ^{14}C "age" of about 37,500 years BP and a $\delta^{13}C_{PDB}$ value of −25.69‰ consistent with terrestrial plant organic carbon, and ruling out contamination. A nearby leaf imprint in the basalt was identified as probably *Lauraceae*. The olivine basalt yielded an averaged K-Ar "model age" of 47.5 Ma, excessively older than the expected "age" of 30 Ma due to excess $^{40}Ar^*$.

The basalt's incompatible trace and rare earth element, and Nd-Sr isotope, geochemistry are consistent with its tectonic setting, being an intraplate continental alkali basalt derived from a homogeneous mantle source and erupted as the Australian plate moved northwards over a stationary hotspot. A Pb-Pb isotopic linear array which gives an apparent "age" of 5.07±0.27 Ga is probably a primary geochemical feature of the basalt's mantle source.

In the context of the Creation/Flood model of earth history the fossilized wood is from trees which grew in the immediate post-Flood period. The decelerating Australian plate drifted over a mantle hotspot, a structural weakness in the crust allowing magma to erupt as basalt which engulfed the trees. The fossilized wood's radiocarbon demonstrates the basalt's youthfulness and the failure of radioisotopic "dating," but is consistent with a Flood/immediate post-Flood stronger magnetic field.

Keywords

Fossilized Wood, Basalt, Crinum, Melaleuca, ^{14}C, K-Ar Model Age, Geochemistry, Isotopic Analyses, Biblical Flood Model

Introduction

The Crinum Colliery, situated near Emerald in the Bowen Basin of central Queensland (Figure 1), was developed to exploit the Lilyvale (German Creek) Seam of the Permian German Creek Coal Measures. During construction of the mine by B.H.P. Australia Coal Pty. Ltd. in 1993, when Shaft Sinking and Development employees were sinking the upcast ventilation shaft, a rare find was made (Anonymous, 1993). After digging through the thin surficial sands and clays, followed by Tertiary basalt, 21 m down pieces of fossilized wood were found entombed in the basalt near the base of the flow. The basalt flow unconformably overlies the uppermost siltstone and sandstone units of the German Creek Coal Measures (Devey, 1995).

The excavators reported at the time that the fossilized wood appeared to belong to two distinct trees, partly standing, still organic in nature and thus not fully petrified (Anonymous, 1993). The imprint of a leaf was also discovered within the basalt, which was also regarded as remarkable, given the likely temperature (perhaps as high as 1000°C) of the basalt lava when it entombed the leaf (and the wood). Additionally, what looked like tree roots were found in the siltstone directly below the basalt, suggesting the trees when alive were rooted into the Permian siltstone and thus growing on a Tertiary land surface over which the basalt lava flowed (Chalmers, 1994).

The investigations reported here focussed on:

1. identifying the trees represented by the fossilized wood and leaf impression, and testing the wood for a possible ^{14}C "age," which might be expected if these were trees growing on a Tertiary (post-Flood?) land surface; and
2. characterizing the geochemistry of the basalt enclosing the fossilized wood, and determining the "age" and source of the basalt by its K-Ar, Rb-Sr, Sm-Nd, and Pb-Pb radioisotopic systematics.

Local Geology

The exposed Bowen Basin (Figure 1, inset) is the northern section of the 1800 km long Bowen-Sydney Basin, a meridional accumulation of Permian and Triassic sediments in eastern Queensland and New South Wales (Staines & Koppe, 1980). Exposures of Bowen Basin sediments extend over an area of 550 km north-south by 250 km across (east-west). Around the western, northern, and eastern margins of the basin the Permian sediments onlap the pre-

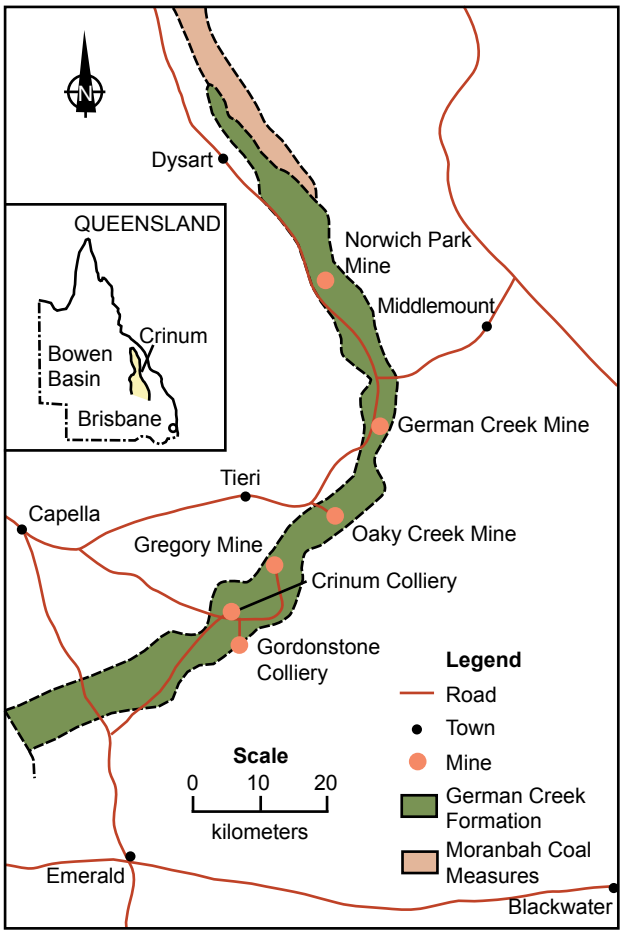

Figure 1. Map showing the location of the Bowen Basin in central Queensland (inset) and the Crinum Colliery north of the town of Emerald (after Devey) (Falkner, 1993).

Permian basement, whereas to the south the Bowen Basin sediments themselves disappear beneath the Jurassic-Cretaceous Surat Basin of southern Queensland.

The Crinum area is about 50 km by road north-northwest of the town of Emerald at approximately 148°19′E, 23°12′S (Falkner, 1993; Olgers, 1984) (Figures 1 and 2). The pre-Permian basement to the west of Crinum consists of schist, phyllite, quartzite, slate, and recrystallized limestone of the Anakie Metamorphics, overlain further west by the Devonian-Carboniferous sediments and acid flows and tufts of the Drummond Basin (Olgers). To the west of Crinum the Permian sediments of the Bowen Basin unconformably overlie the basement metamorphics of the Anakie Inlier, an erosional remnant preserved as a ridge.

The complete Permian stratigraphic sequence of the Bowen Basin is not represented in the Emerald-Crinum area. Also, since the original field mapping and during subsequent mining operations, there have been difficulties in correlating strata across such a large basin, and thus variations in the identification and naming of strata have resulted (Mallett et al., 1995; Park, 1975). Nevertheless, the original broad groupings and subdivisions of strata continue to be used and are represented in the Emerald-Crinum area. Thus the first strata to be deposited belong to the Upper Permian Blenheim Sub-Group of the Back Creek Group—about 365 m of quartz and lithic quartz sandstones, conglomerate, and micaceous and carbonaceous mudstone, containing marine fossils (brachiopods and pelecypods), which outcrop to the north and west of Crinum (Olgers, 1984) (Figure 2). These strata are overlain by 610 m or more of quartz sandstone, sandstone, carbonaceous siltstone and mudstone, coal seams, and conglomerate of the German Creek Coal Measures of the Back Creek Group (Olgers). Outcrops occur in a strike-oriented belt immediately to the north-east of Crinum, but this coal measure sequence continues to the south-west underneath Tertiary basalt flows at Crinum and Gordonstone and under soil, gravel and alluvium cover (Falkner, 1993; Olgers) (Figures 1 and 2). To the south-west of Crinum and west of Emerald beyond the basalt, soil, gravel, and alluvium cover are outcrops of undifferentiated Back Creek Group strata (Figure 2)—about 1370 m of quartz and pebbly quartz sandstones, feldspathic and micaceous sandstone, and mudstone containing marine fossils (brachiopods, pelecypods, and gastropods), and some coal seams (Olgers). On the other hand, directly overlying the outcropping German Creek Coal Measures east of Crinum are more than 610 m of lithic and feldspathic sandstone, conglomerate, tuff, tuffaceous sandstone, and mudstone strata of the Fair Hill Formation of the Blackwater Group which contain petrified wood and poorly preserved plant remains.

The occurrence of the coal seams interbedded with clastic sediments containing marine fossils poses a challenge to the uniformitarian framework for interpreting the supposed sedimentary environments in which these strata were deposited (Fielding, Stephens, Kassan, & Holcombe, 1995). Thus the depositional basin is interpreted as a shallow marine shelf onto which clastic sediments were deposited by rivers flowing from the presumably exposed land to the west, burying marine animals. On the coastal and alluvial plains it is claimed wetlands developed into coal-forming swamps before slow subsidence allowed the sea to encroach and bury the peat. These coal measures were supposedly deposited by such cyclical repetition until the marine shelf was subsequently totally filled and covered over with fluvial sediments washed in from the north with wood and other plant debris. Alternately, during the global Flood cataclysm the plant debris would have been catastrophically accumulated and buried by the sedimentation within the globe-encircling marine environment.

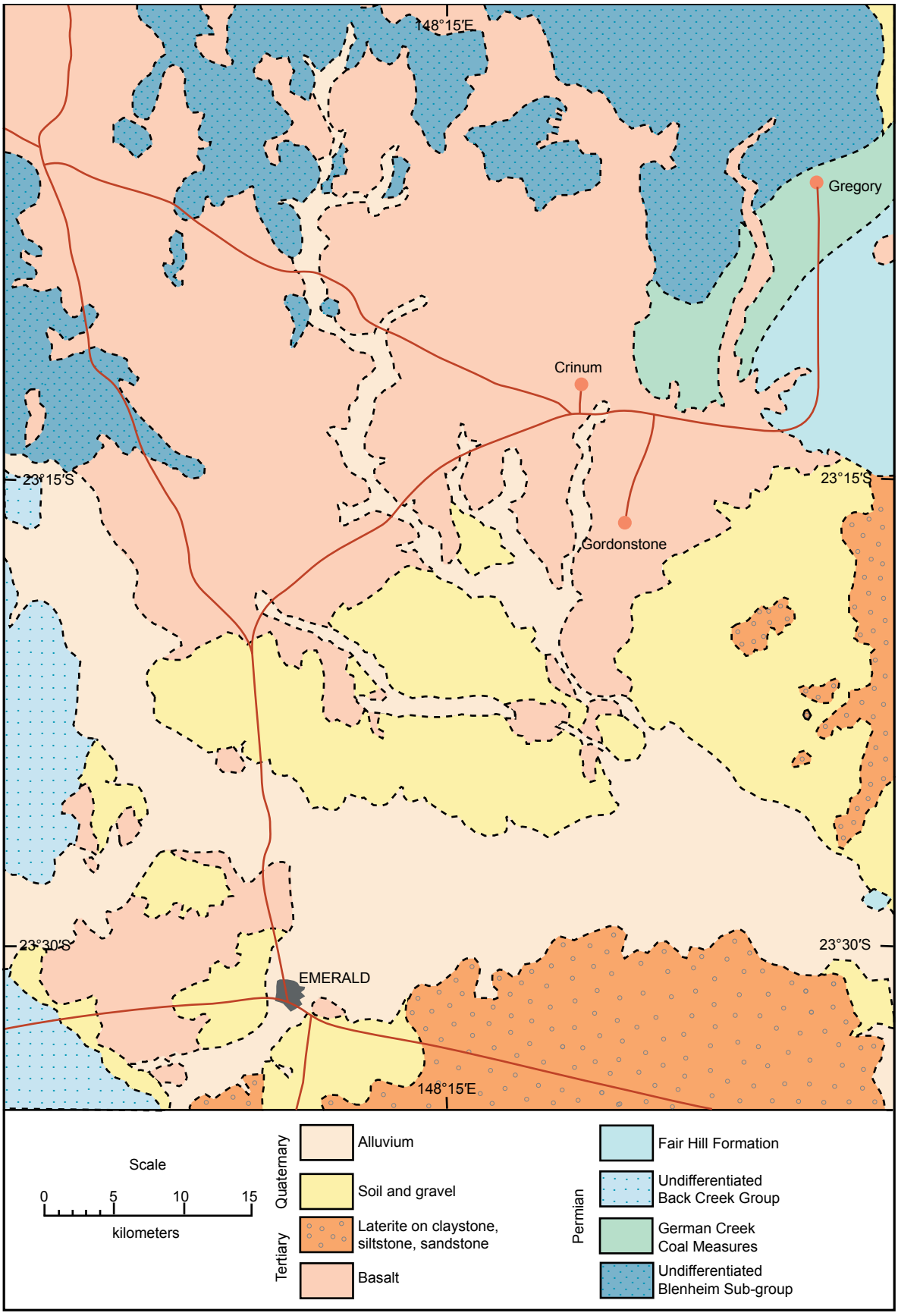

Figure 2. Geological map of the Crinum-Emerald area [*Olgers*, 1984].

By the end of the Permian it is claimed sedimentation had ceased in the Emerald-Crinum area as the shallow sea retreated eastward (Fielding et al., 1995). Through the entire Mesozoic the area was supposedly a land surface at which presumably the exposed strata were weathered and eroded. Then in the Tertiary, intense volcanic activity to the west resulted in extensive olivine basalt flows being extruded eastwards across the area, building up a cumulative thickness in places of up to 245 m (Olgers, 1984). Interbedded with the basalt flows are layers of claystone, siltstone, sandstone, pebbly sandstone, and gravel, up to 105 m thick in total, interpreted as fluvial and lacustrine sediments. Subsequent intense weathering has produced a laterite capping on these Tertiary sediments, which can be seen in outcrop to the south-east and south of Crinum (Olgers) (Figure 2). And finally, continued in situ weathering accompanied by fluvial processes have not only shaped the present landscape, but left thin blankets of superficial soil, sand, gravel, and alluvium covering all earlier strata, particularly in low-lying areas.

Mine Geology

The Crinum Colliery has been sited and developed to exploit the Lilyvale Seam of the German Creek Coal Measures (Falkner, 1993) (Figures 1 and 2). The immediate mine area is in a relatively undeformed and stable region, the coal measure sequence in the mine lying on the western limb of a gently dipping syncline which gently plunges south-west (Devey, 1995). The regional dip is generally about 3° to the south and south-east.

Figure 3 is a simplified longitudinal, west-to-east cross-section through the Crinum Mine drift entries. Flat-lying Tertiary clay and basalt flows unconformably overlie the gently folded and dipping Permian strata, and are generally 20–40 m thick. As many as eight distinct basalt flows have been recognized in the nearby Gordonstone area to the south (Devey, 1995) and these are often interbedded or underlain by clay, as is the case at Crinum (Figure 3).

The German Creek Seam, and its lateral equivalent at Crinum, the Lilyvale Seam, forms the base of the upper German Creek Coal Measures, which average 160 m in thickness (Falkner, 1993). The seam is generally between 3.0 and 4.5 m thick, averaging 3.5 m at Crinum, has only a few thin claystone partings, is vitrinite-rich, low in ash and sulphur, and has excellent coking properties. There are other seams in the upper German Creek Coal Measures above the German Creek (Lilyvale) Seam (in stratigraphic order upwards—the Corvus, Tieri, Aquila, and Pleiades Seams), but these are generally thinner or absent in the Crinum area. The upper German Creek Coal Measures are dominated by quartz lithic sandstone, with minor siltstone interbeds (as in Figure 3), which have been interpreted as eight separate lithofacies in what was supposedly a fluvial delta depositional environment prograding onto a shallow marine shelf. Thus the lower German Creek Coal Measures, which average 110 m thick, do not contain economic coal and are interpreted as a marine sequence.

Discovery Location

Whereas large-scale open cast strip mining methods have traditionally been utilized to exploit the German Creek (Lilyvale) Seam to the north-east at the Gregory, Oaky Creek, and German Creek Mines (Figure 1) where the overburden is shallow, (Mallett et al., 1995) at Crinum the seam is deeper

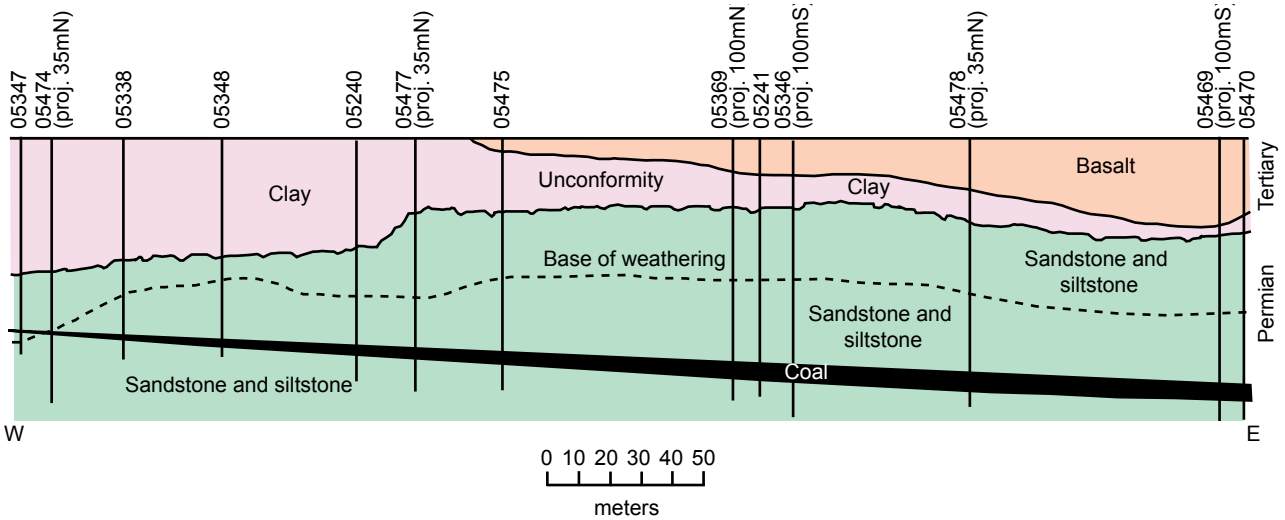

Figure 3. Simplified longitudinal, west-to-east cross-section through the Crinum Mine drift entries showing the geology and exploratory drill-holes (adapted from the B.H.P. Australia Coal Pty. Ltd.'s Crinum Mine Project cross-section.) The upcast ventilation shaft was excavated in the approximate position of Drill-hole 05469.

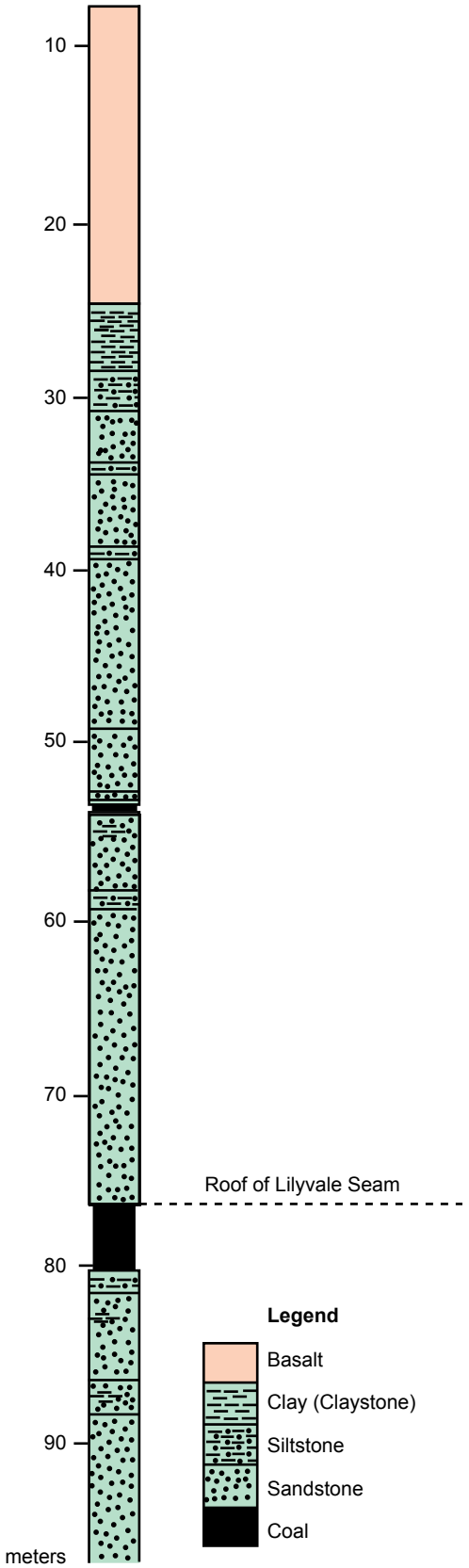

Figure 4. Geological log for Drill-hole 05469 showing the strata sequence intersected by the upcast ventilation shaft (adapted from the B.H.P. Australia Coal Pty. Ltd.'s Crinum Mine project drill-hole log.)

and so underground longwall mining methods are being used. Drilling preceded development so that planning could optimize the siting of the transport and conveyor drifts, and the upcast ventilation shaft, with respect to the longwall production panels in the seam (Chalmers, 1994). Thus the drifts were excavated along the mine section shown in Figure 3, and the upcast ventilation shaft alongside Drill-hole 05469 just 100 m south of that section.

It was during the sinking of the upcast ventilation shaft in 1993 that the excavators found the fossilized wood entombed in the Tertiary basalt flow (Anonymous, 1994). The strata sequence in the shaft as recorded by Drill-hole 05469 is shown in Figure 4. The excavators reported finding the pieces of fossilized wood at about 21 m down the shaft in the bottom flow of the sequence of Tertiary basalt flows. At approximately 4 m thick, this basalt flow was reported to consist of three distinct sections—lots of vesicles in the "frothy" top of the flow, then below that, coarser basalt with visible phenocrysts and perhaps some columnar jointing, and at the bottom of the flow, fine-grained, dense, hard, massive basalt (Anonymous, 1993; Chalmers, 1994). Being relatively thin with such an internal structure, cooling of this flow would have been rapid (perhaps days, but a few weeks at most) (Snelling, 1991). While Figures 3 and 4 show that there is clay/claystone immediately below the basalt, careful examination of the core recovered from Drill-hole 05469 revealed that the basalt sits at 25.2 m downhole unconformably and directly on the Permian strata of the German Creek Coal Measures. There is no "fossil soil" but a hard, dense, silicified claystone/fine-grained siltstone, grading downwards into siltstone then sandstone. The roof of the Lilyvale Seam is then at 76.5 m downhole, only 51.3 m below the base of the bottom basalt flow which entombed the fossilized wood.

What was Found

The workmen sinking the shaft reported that they found two distinct trees, still standing, partly organic in nature, and thus not fully petrified (Anonymous, 1994). Because the fossil wood specimens they collected were said to have come from a depth in the shaft of about 21 m, the basalt flow entombing the trees is about 4 m thick (Chalmers, 1994), the bottom of the basalt flow in the drill-hole is at 25.2 m and also encases fossilized wood, and what appear to be thick petrified roots were found in the siltstone below (Chalmers), then these appear to have been tree stumps over 4 m tall entombed through the full thickness of the basalt flow. (The apparent lack of any preserved "fossil soil" is not altogether unexpected, given that trees are capable of growing on rocky outcrops.) Thus the fossilized wood samples the

Figure 5. One of the pieces of fossilized wood recovered from the basalt flow during excavation of the upcast ventilation shaft (the pen is for scale.) The outer areas that were in contact with the hot basalt lava have been burnt to white ash. (Courtesy of B.H.P. Australia Coal Pty. Ltd.'s Crinum Mine Project.)

Figure 6. Another of the pieces of fossilized wood, showing black charring where it was in contact with the hot basalt lava (the pen is for scale.) Courtesy of B.H.P. Australian Coal Pty. Ltd.'s Crinum Mine Project.)

Figure 7. Another piece of the fossilized wood recovered during excavation of the upcast ventilation shaft, showing some basalt still attached to its charred outer surface (the pen is for scale.) (Courtesy of B.H.P. Australia Coal Pty. Ltd.'s Crinum Mine Project.)

Figure 8. A completely sharred piece of the fossilized wood recovered from the basalt (the pen is for scale.) (Courtesy of B.H.P. Australia Coal Pty. Ltd.'s Crinum Mine Project.)

Figure 9. Another piece of the fossilized wood which shows very little charring. The fossilized wood itself is brown, probably due to impregnation with iron minerals during fossilization (the pen is for scale.) (Courtesy of B.H.P. Austrlian Coal Pty. Ltd.'s Crinum Mine project.)

Figure 10. The piece of basalt with the imprint of a leaf on its surface. The leaf itself was not preserved and the basalt is stained with iron minerals, but the leaf imprint is still intact (the pen is for scale.) (Courtesy of B.H.P. Australia Coal Pty. Ltd.'s Crinum Mine Project.)

workmen collected probably came from near the tops of the tree stumps at the top of the basalt flow, which is verified by the vesicular nature of the basalt sample they also collected at the same location, the top of the basalt flow having been described as vesicular.

The fossilized wood when found was said to be in three states—ash, charred, and intact timber (Anonymous, 1994). Because the original trees appear to have been rooted into the Permian strata (Chalmers, 1994) and thus growing on a Tertiary land surface, now preserved as the unconformity between the Permian strata and the Tertiary basalt (Figure 3), it is not surprising that when the molten basalt lava at 1000–1200°C engulfed the trees some of the wood was reduced to ash or was charred. In fact, it is likely that the charring of the outer sections of the tree stumps protected the inner portions. The pieces of fossilized wood collected by the workmen are shown in Figures 5–9, and the effects of charring can readily be seen. The imprint of a leaf (Figure 10) was also discovered in the basalt, indicative of how quickly the molten lava congealed. Close inspection reveals that it is not a "gum leaf," as initially reported (Anonymous, 1994). Finally, as already mentioned, what clearly appear to be thick petrified/fossilized roots related to the trees were found in the Permian siltstone immediately underneath the Tertiary basalt entombing the fossilized wood (Chalmers, 1994), and a sample was collected by the workmen (Figure 11).

Collection of Samples

Contact was made with the mine staff expressing an interest in investigating their discovery. Small fragments of some of their fossilized wood samples were received, and a visit to the mine took place on August 31, 1994. The pieces of fossilized wood recovered by the workmen were examined and photographed, as too was the leaf imprint in the Tertiary basalt sample and the fossilized roots in the

Figure 11. The apparent fossilized tree roots in a piece of the Permian siltstone recovered during excavation of the upcast ventilation shaft (the pen is for scale.) (Courtesy of BHP Australia Coal Pty Ltd's Crinum Mine Project.)

Figure 12. Drill core from Drill-hole 05469 (courtesy of BHP. Australia Coal Pty Ltd's Crinum Mine Project.) In the center of the photograph is a piece of charred fossilized wood entombed in the very bottom of the Tertiary basalt (to the left and in the next row above) right at the boundary at 25.2 m with the Permian siltstone (to the right.)

Permian siltstone sample (Figures 5–11). However, access to the ventilation shaft was not possible, nor were samples of the basalt directly enclosing the fossilized wood available, having long been dumped with all the other rubble and waste rock.

Nevertheless, during the mine visit it was realized that an exploratory hole had been drilled close to where the shaft had been sunk (Chalmers, 1994). The relevant drill core from Drill-hole 05469 was found, and upon inspection, it contained pieces of fossilized wood, still apparently containing organic carbon, at the bottom of the lowermost basalt flow, encased in the basalt at the boundary of the Tertiary basalt with the Permian siltstone below (Figure 12). This drill core was later provided by the mining company for use in this investigation.

During the mine visit it was noted that the site was devoid of outcrops. However, about 3 km southeast of the mine site large outcrops of the Tertiary basalt were found beside a waterhole in Crinum Creek (Figure 2). Even though these outcrops probably represent a different (younger) basalt flow to the one that entombed the wood, they were sampled to provide a comparison with the basalt in the drill core, one sample of vesicular basalt from near the top of the main outcrop, and a second sample of massive basalt from vertically halfway down the same large outcrop (Figure 13).

Laboratory Work

Fragments of the fossilized wood provided by the mine staff, from the large pieces collected by the workmen while sinking the ventilation shaft, were sent to wood specialist Dr. Geoff Downes, of the CSIRO Division of Forestry and Forest Products, for identification of the species. Additionally, an enlarged

Figure 13. Large outcrop of Tertiary basalt beside the waterhole in Crinum Creek near the Crinum Colliery. Two samples of basalt were collected from this outcrop.

photograph of the leaf imprint in the basalt was circulated to several paleobotanist for identification.

At the C.S.I.R.O. laboratory a piece of the fossilized wood was taken from the least heat affected region of the sample and examined by incident light microscopy, as well as by Field Emission SEM. Efforts were made to section the fossilized wood, but permineralization was too advanced. A Leica DRM-RXE light microscope was used to examine fractured and polished surfaces to identify features of taxonomic importance. Transverse and radial longitudinal surfaces (Figure 14) had been polished using a range of abrasive cloths down to 2400 grit. Both incident darkfield and polarized light were then used in an effort to find features that would enable identification of the wood. Additionally, a Phillips Field Emission SEM with an accelerating voltage of less than 10 kV was used to examine fractured surfaces.

Other small fragments from the fossilized wood samples found during sinking of the ventilation shaft were sent for radiocarbon (^{14}C) analyses to two reputable laboratories, one set of different fragments to each laboratory. The same radiocarbon laboratories were also sent tiny portions of the same piece of fossilized wood found encased at the base of the same basal basalt flow 25.2 m down Drill-hole 05469. Neither Geochron Laboratories in Cambridge, Boston (USA) nor the Antares Mass Spectrometry Laboratory at the Australian Nuclear Science and Technology Organisation (ANSTO), Lucas Heights near Sydney (Australia), was told where the samples came from to ensure that there would be no resultant bias. Both laboratories use the more sensitive and reliable accelerator mass spectrometry (AMS) technique for detecting radiocarbon. Geochron is a commercial laboratory and Antares is a major research laboratory.

Two pieces each of the basalt samples from the drill core (from the flow which enclosed the fossilized wood) and the outcrop were submitted to the AMDEL Laboratories in Adelaide (Australia) for major, minor, and trace element analyses. Further sample pieces were sent to the AMDEL Laboratories and Geochron Laboratories for conventional K-Ar dating, and to the PRISE Laboratory in the Research School of Earth Sciences at the Australian National University in Canberra (Australia) for Rb-Sr, Sm-Nd, and Pb-Pb isotopic determinations. AMDEL Laboratories is a reputable commercial laboratory employing the latest conventional analytical equipment and techniques such as inductively coupled plasma emission spectroscopy (ICP), while the PRISE Laboratory utilizes all the state-of-the-art and innovative mass spectrometry technology of a university research school with an outstanding international reputation.

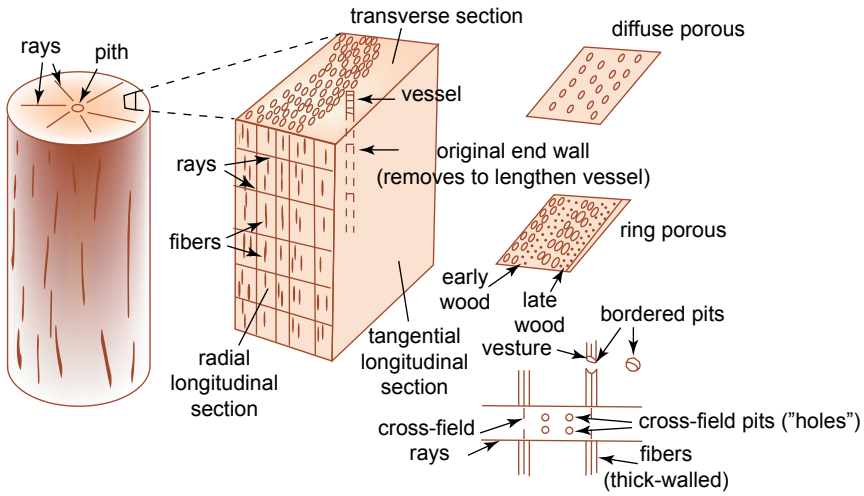

Figure 14. Diagram to illustrate the terminology used to describe the anatomical features of woods, including the types of sections which are cut for microscopy.

Results

Wood identification (with G. Downes)

Figure 14 provides a diagrammatical explanation of some of the terminology used to describe the anatomical features of woods which can be diagnostic of the family, genus, and sometimes species to which they belong. The essential components are the vessels, rays and fibres. Vessels are formed from individual vessel elements which are single cells produced in the vascular cambium. Each cell dies after enlargement and maturation, a part of this process being the removal of the end

walls, connecting it with other elements. A long tube or vessel is formed, through which xylem sap passes as part of the transpiration stream. Vessels are orientated axially and form cross-fields where they intersect radially-orientated rays. Within these intersections, or cross-fields, pits or "holes" occur, the arrangement of which varies between taxonomic groups. Similar cross-fields occur where rays cross axially-orientated fibers. The spacing of the vessels and their diameters relative to one another are also diagnostic. For example, vessels can vary from an even spacing of equidiameter vessels common in eucalypts (diffuse porous), to closely-packed rings of large-diameter vessels ("early wood") alternating with small-diameter ("late wood") found in oaks (ring porous). Adjacent thick-walled fibers form bordered pits. Certain hardwoods have vestures, which are small occlusions occurring within the pit borders. The thin-walled cells that are relatively undifferentiated or unspecialized infilling between the vessels are called parenchyma, and the pattern of the occurrence of parenchyma tissue can also be taxonomically important.

The fossilized wood was identified as most probably belonging to the genus *Melaleuca,* which is in the *Myrtaceae* family that includes the eucalypts. However, features which would enable a more definitive identification were not found. The fossilized wood was a diffuse porous hardwood. Ray-to-vessel pitting was found to be simple, with several pits per cross-field. Bordered pit apertures appeared to be occluded, perhaps with silica (SiO_2). The important parameters measured and described by light microscope study of the fossilized wood are:

Fiber length	700–800 µm A lot of parenchyma; elongated; axial. Some possibly vasicentric tracheids.
Vessel diameters	40–100 µm
Vessel frequency	~10 per mm^2
Bordered pits	~5 µm diameter
Vessel-to-ray pitting	several small, simple pits per cross-field
Narrow uniseriate rays	(therefore, not *Casuarina)*
Rays	200–300 µm high in tangential longitudinal section commonly 6–10 cells high

Unfortunately, it could not be determined whether the bordered pits had vestures, which would be further diagnostic of *Melaleuca.*

Figures 15 to 25 are Field Emission SEM photomicrographs illustrating some of the anatomical features found in the Crinum fossilized wood. The resolution possible with the Field Emission SEM system operating at low accelerating voltages enabled resolution of the microfibrillar structure in the cell walls (Figure 18). The tendency of the fossilized wood to fracture along the middle lamella/primary wall interface (Figures 15, 18–20) allowed the microfibril orientation of the primary wall to be seen. In places the fracture extended to the surface of the secondary wall (Figures 18 and 19). The angle of the pit aperture is probably indicative of the microfibril angle of the S2 layer of the secondary wall. The circular orientation of the microfibrils around the bordered pit is evident (Figures 18 and 20), the pits being around 5µm diameter.

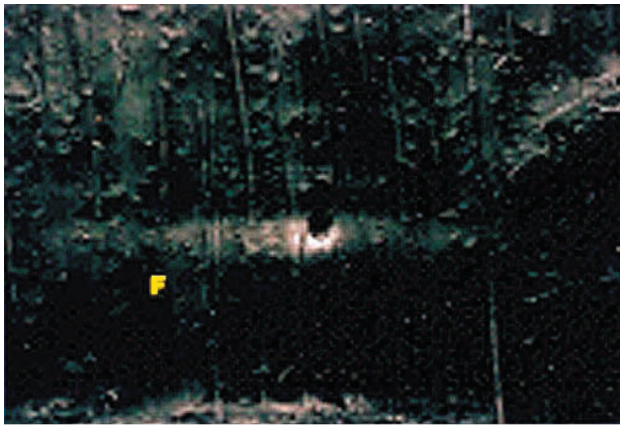

Figure 15. Field emission SEM photomicrograph of a radial longitudinal section through the fossilized wood showing wood fibers (F). Apparent decay of the middle lamella region resulted in fracture through this wall layer, exposing the primary wall. Evidence of bordered pits along fibers is abundant. (Courtesy of G. Downes.)

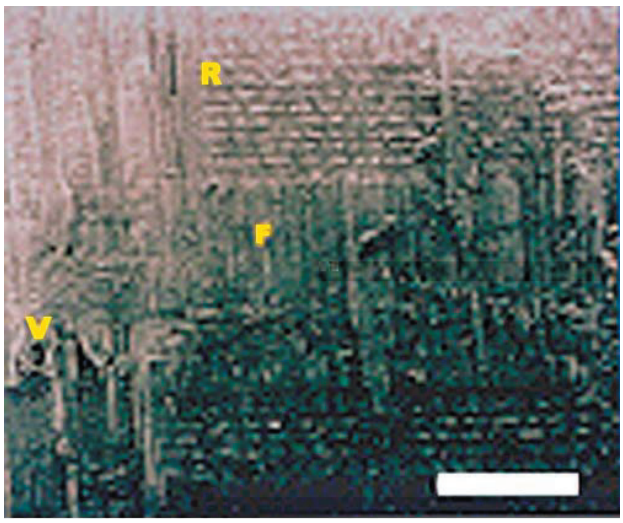

Figure 16. Field emission SEM photomicrograph of another radial longitudinal section through the fossilized wood. Exposed on this face are ray (R) and fiber (F) cross-fields. Vessel (V) elements are evident to the left. Bar=200 µm. (Courtesy of G. Downes.)

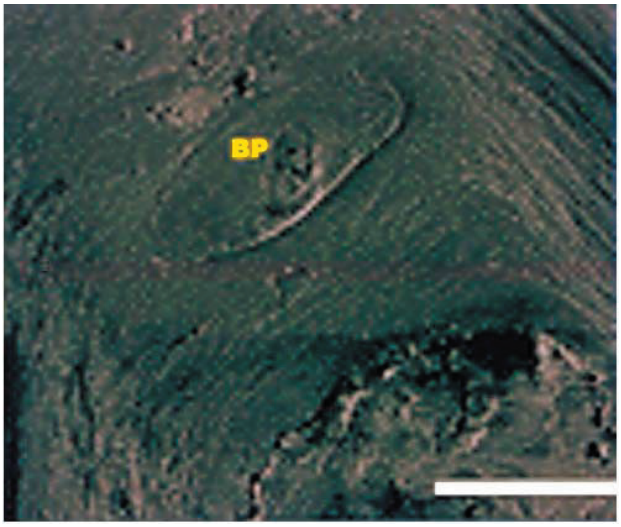

Figure 17. Field emission SEM photomicrograph of a fracture surface of the fossilized wood. Bordered pits are well preserved, with the fracture usually along the middle lamella region, exposing the internal pit face. Bar=2μm. (Courtesy of G. Downes.)

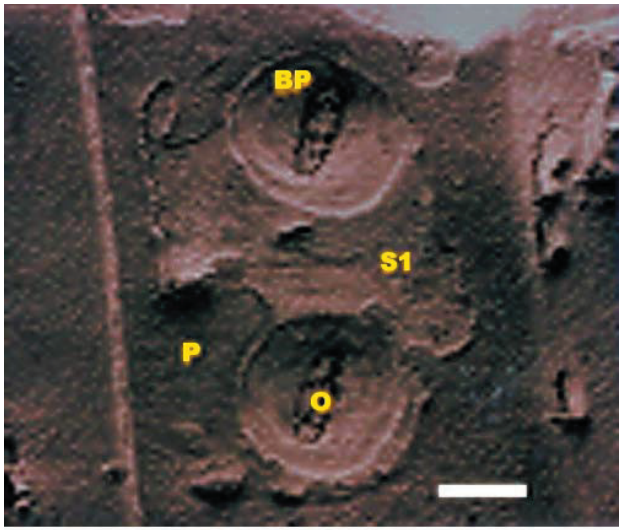

Figure 18. Field emission SEM photomicrograph of the fossilized wood showing that cellulose microfibril orientation is preserved, and the changes in orientation associated with the bordered pits (BP), the primary wall (P) and the S1 layer of the secondary wall. Occlusions (O) in the pit apertures are ubiquitous. Bar=2μm. (Courtesy of G. Downes.)

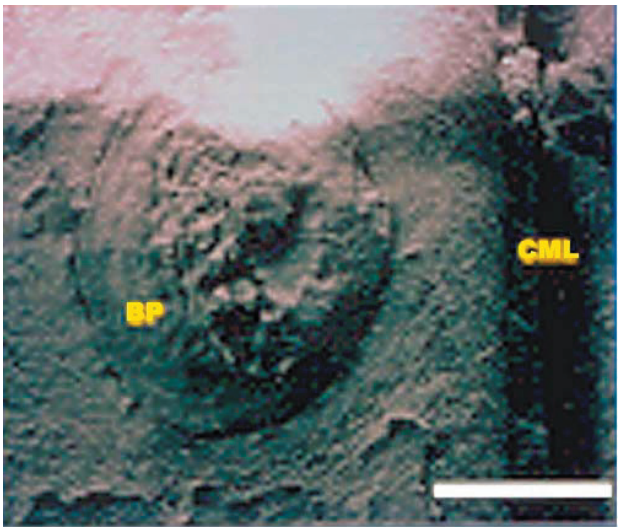

Figure 19. Field emission SEM photomicrograph of the fossilized wood showing the reverse face of a bordered pit (BP) together with the aperture. The compound middle lamella (CML) is exposed, with the inner face of the secondary wall being evident. Bar=2μm. (Courtesy of G. Downes.)

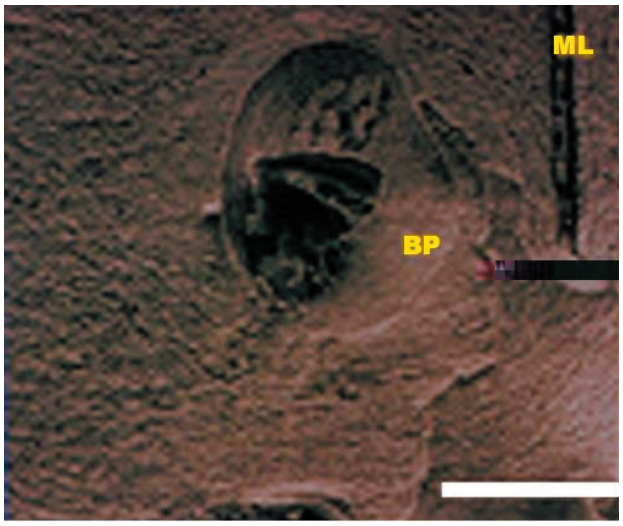

Figure 20. Field emission SEM photomicrograph of the fossilized wood showing that microfibril orientation in and around a bordered pit (BP) is preserved. The compound middle lamella (ML) region between adjacent fibers is evident. Bar=2μm. (Courtesy of G. Downes.)

An analysis of the chemical composition of the Crinum fossilized wood by SEM-EDS (Energy Dispersive System) indicated that carbon and oxygen were still present (Figure 25). However, the presence of silicon was also evident, suggesting that the original wood had undergone a considerable degree of permineralization, which would thus be principally silica (SiO_2).

Leaf Identification

Identification of the leaf imprint in the basalt (Figure 10) proved straightforward. When seen in the enlarged photograph by palaeobotanists M.E. White (consultant) and M. Pole (University of Queensland) the fossilized leaf was readily identified as belonging to the family *Lauraceae*.

For comparison, in Figure 26 is a reproduction

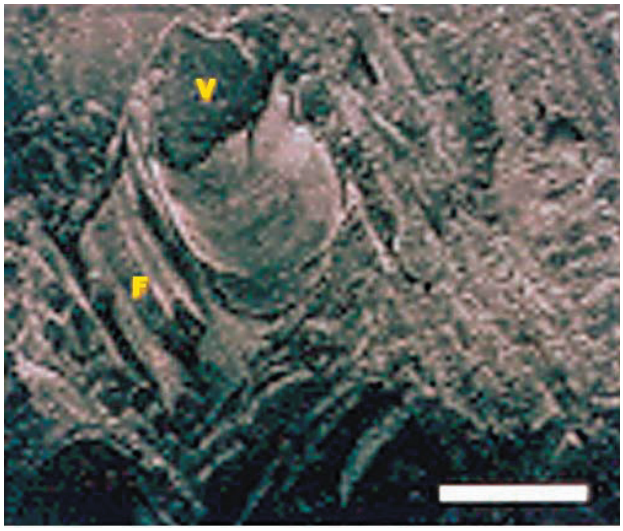

Figure 21. Field emission SEM photomicrograph of the fossilized wood showing vessel (V) elements and fibers (F) in a fractured transverse surface. Bar=50µm. (Courtesy of G. Downes.)

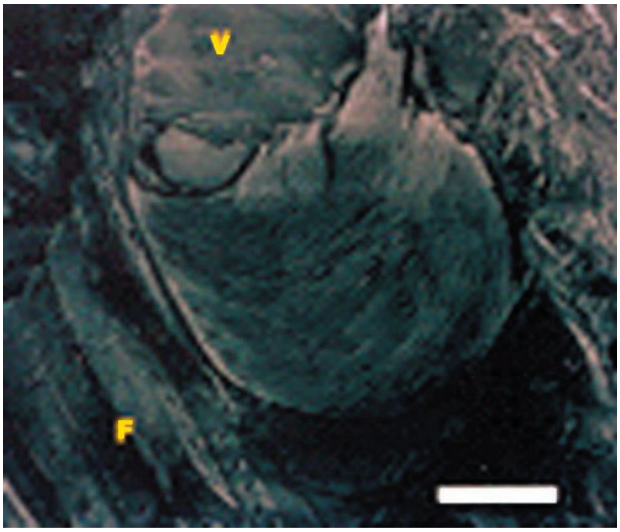

Figure 22. Field emission SEM photomicrograph of the fossilized wood showing a closer view of a fractured vessel (V) and fibers (F). The pitting along the vessel wall is apparent. Bar=20µm. (Courtesy of G. Downes.)

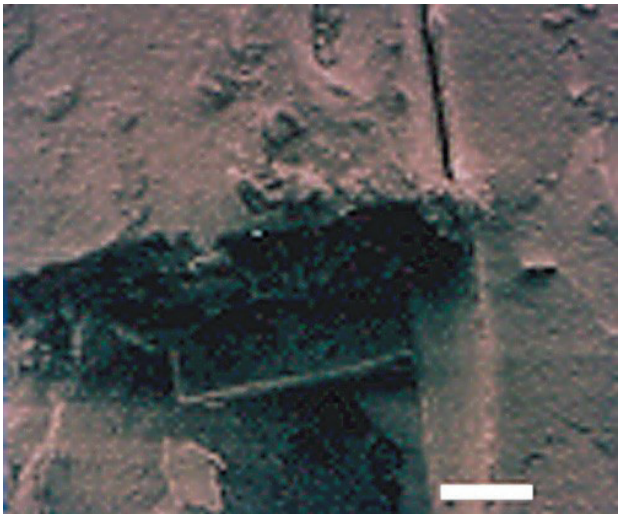

Figure 23. Field emission SEM photomicrograph of the fossilized wood showing two adjacent fibers slightly separated along the middle lamella. The left fiber has fractured transversely. Bar=2mm. (Courtesy of G. Downs.)

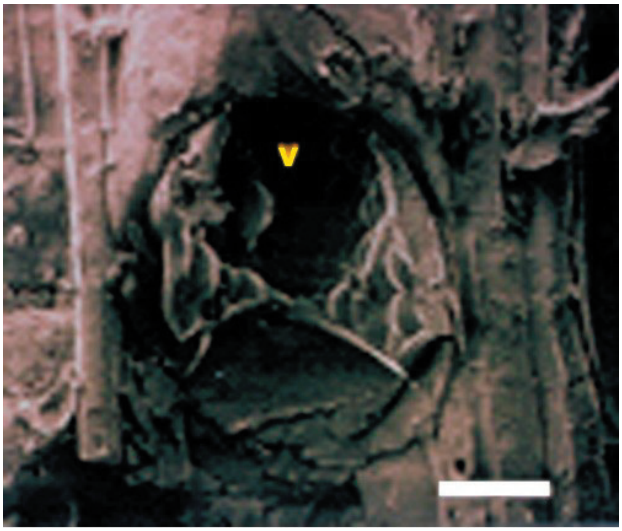

Figure 24. Field emission SEM photomicrograph of the fossilized wood showing a vessel (V) element with the remains of smooth vesicle-like structures, possibly tyloses. Bar=20mm. (Courtesy of G. Downes.)

of a fossilized *Laurophyllum conspicuum* leaf from Nerriga in New South Wales, Australia (140km east of Canberra) (Hill, 1986). The crucial similarities are the venation and the leaf shape. Furthermore, fossilized *Lauraceae* leaves have been reported from Moranbah in the northern Bowen Basin (Christophel, 1994), so this fossilized leaf at Crinum is not "out-of-place." The fact that the original leaf appears to have belonged to a totally different tree to that from which the fossilized wood came does not invalidate the identification, because a vegetated environment normally has a variety of trees.

Wood radiocarbon (^{14}C)

The radiocarbon (^{14}C) results are listed in Table 1, and reveal that detectable radiocarbon was found in all fossilized wood samples. The results are within the detection limits of the analytical equipment and

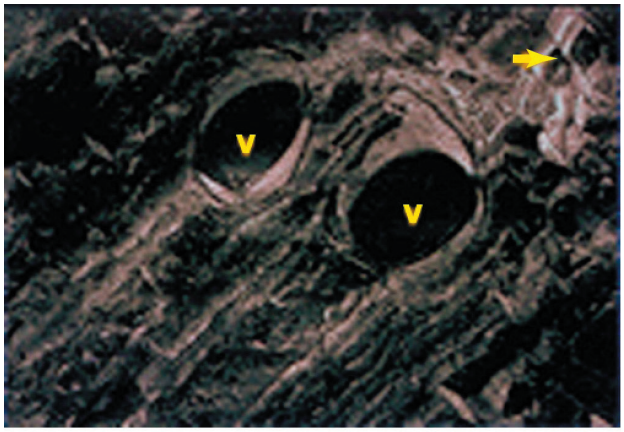

Figure 25. Field emission SEM photomicrograph of the fossilized wood showing the fractured region of the transverse surface and the preservation of vessel (V) elements. Individual fibers can also be resolved (small arrow.) EDS analyses in these regions indicate the presence of silicon, oxygen, and carbon. (Courtesy of G. Downes.)

Figure 26. A reproduction of a fossilized leaf of Laurophyllum conspicuum from Nerriga, New South Wales, Australia (after Hill, 1986). Scale bar = 1 cm.

therefore provided finite "ages." The one exception was obviously due to the small quantity of carbon extracted from the sample, but the parallel analysis at the other laboratory on the same piece of fossilized wood from the basalt in the drill core returned a finite "age." The laboratories' staff when questioned had neither hesitation nor difficulties in calculating the quoted ^{13}C-corrected radiocarbon "ages," which they staunchly defended as valid. Thus the ^{14}C "age" of the fossilized wood from the drill core would appear to be 44,000–45,500 years BP, whereas the fossilized wood samples from the ventilation shaft appear much younger. The age differences in Table 1 are incongruous, given that the fossilized wood is supposed to have all been derived from the same trees, but the quantities of carbon analyzed being so small might result in such large variations. Perhaps an averaged age would be more appropriate, and that would give the fossilized wood a radiocarbon "age" of around 37,500 years BP.

The possibility of contamination is also an important consideration which was raised with the laboratories' staff. For example, recent microbial and fungal activity long after the wood was buried, including spores and dust in the laboratories, might have contaminated the fossilized wood with various amounts of radiocarbon to produce these different ^{14}C "ages." However, the responses were unhesitatingly unanimous that there would be no such contamination problem (Krueger, 1996; Lawson, 1996). Modern fungi or bacteria in fact derive their carbon from the organic material they live on and don't get it from the atmosphere, so they would have the same "age" as their host (Krueger). Furthermore, the lab procedure followed in sample preparation would remove the cells and any waste products from either fungi or bacteria. Samples are treated first with hot dilute hydrochloric acid to remove any carbonates, and then with hot dilute caustic soda to remove any humic acids or other organic contaminants (Wilcox, 1996). After subsequent washing and drying, they are combusted to recover carbon dioxide for the radiocarbon analyses.

However, pieces of the same fossilized wood from the basalt in the drill core, and also pieces of the fossilized wood recovered during excavation of the ventilation shaft, were analyzed by each laboratory and the results are comparable. The radiocarbon "age" depends on the amount of residual radiocarbon left in the sample from the time of its incorporation in the growing wood. This is usually expressed as "percent modern carbon," which is how

Table 1. Radiocarbon (^{14}C) Analyses of the Crinum fossilized wood samples.

Sample	Lab	Lab Code	Conventional ^{14}C Age		$\delta^{13}C_{PDB}$ (‰)
			Age (years BP)	1σ error	
Wood in Drill Core	Geochron ANSTO	GX-20798-AMS OZB472	>35,620 44,700	— 950	–25.7 –25.78
Other Wood	Geochron	GX-20087-AMS	29,544	759	–25.1
Other Wood	ANSTO	OZB473	37,800	3,450	–26.16

Notes: (1) Ages quoted are ^{14}C ages not calendar ages.
(2) The Geochron dates are based on the Libby half-life (5570) years for ^{14}C. The errors stated are ±1σ as judged by the analytical data alone. Their modern standard is 95% of the activity of N.B.S. Oxalic Acid. The ages are referenced to the year AD 1950.
(3) The ANSTO ages have been rounded according to the convention of *Polach and Robertson* [1983.]

much modern carbon it would require to be added to the sample, assuming no ^{14}C to begin with, to yield an "age" equivalent to the calculated radiocarbon "age." It is thus a measure of the sensitivity to sample contamination. In these samples the percent modern carbon was 0.9% and 0.4% for the ANSTO analyses, but between 1.0 and 2.5% for the Geochron analyses. It has been suggested that any unavoidable contamination (laboratory dust and airborne fungal spores) would only amount to at most 0.2% modern carbon, which would have a negligible effect on any analyses of 1.0% modern carbon or more (Hedges, 1998). Thus if such contamination were inadvertently present it would potentially have a noticeable effect on only one of the radiocarbon analyses, but even in that instance the ANSTO laboratory confidently reported the resultant ^{14}C "age" as valid and reliable.

Recent research has focussed on the dating of "old" materials and the problems of contamination (Bird et al., 1999). Radiocarbon analyses of "^{14}C-dead" charcoal from sediments said to be greater than 50,000 years old using the conventional acid-base pre-treatment and single combustion method have yielded "ages" of only 34,820 to 50,360 years, suggesting such pre-treatment was inadequate to remove contamination. However, using a more severe acid-base-wet oxidation pre-treatment and stepped combustion, ^{14}C analyses on the same charcoal yielded "ages" of 37,720 to 55,860 years. This claimed "improvement" is questionable, given that the vague "greater than" 50,000 years "age" for the sediments is based on optically stimulated luminescence (OSL) dating fraught with its own set of difficulties, and not on some external objective standard. Furthermore, the same study found that "geologically ancient," "^{14}C-dead" graphite, even using the same severe pre-treatment, etc., still yielded ^{14}C "ages" of 59,280 to 67,730 years, which was interpreted as perhaps representing the limit attainable due to unremovable sample and lab contamination. Such an interpretation is required, of course, by the uniformitarian bias regarding the "antiquity" of the graphite. On the other hand, it could be that the graphite is not "^{14}C-dead," and the ^{14}C in it is there because the graphite is in fact not all that old. Therefore, such a study neither imposes limits on the supposed antiquity of samples that can be ^{14}C "dated," nor verifies that sample and lab contamination is necessarily still a problem after the appropriate pre-treatment. Thus it cannot be argued that this fossilized wood was too "old" to be ^{14}C "dated," and/or that the ^{14}C "ages" obtained were due to contamination.

Furthermore, whereas there is some variation in the ^{14}C "ages" of the Crinum fossilized wood samples as measured by the laboratories, the reported $\delta^{13}C_{PDB}$ results, the measured differences between the $^{13}C/^{12}C$ ratios in the samples compared to Pee Dee Belemnite (in the last column of Table 1), are extremely uniform. Thus, they are essentially the same, with the average value of –25.69‰ (per mil) being totally consistent with the analyzed carbon in the fossilized wood representing organic carbon from wood which belonged to terrestrial plants (Hoefs, 1997), and not from contamination.

Table 2. Major, trace, and rare earth element analyses of the Crinum basalts. (Units: % major oxides; ppm trace and rare earth elements.)

Sample	BCW-1	BCW-2	BCM-2	BCM-3
SiO_2	55.0	54.5	60.0	61.0
TiO_2	1.42	1.39	1.65	1.68
Al_2O_3	15.0	14.5	17.0	17.5
Fe_2O_3	10.5	9.43	5.07	3.66
MnO	0.14	0.12	0.07	0.05
MgO	4.91	6.30	2.02	1.08
CaO	7.48	7.31	6.98	6.93
Na_2O	3.57	3.57	3.71	3.91
K_2O	0.60	0.59	0.83	0.88
P_2O_5	0.23	0.22	0.20	0.20
Lol	2.22	2.66	3.24	3.77
Total	101.07	100.59	100.7	100.6
Rb	9.5	10.0	19.0	20.5
Sr	220	260	300	340
Y	12	13	13	17
Hf	4	3	3	3
Zr	100	80	100	120
Nb	15	15	20	20
Ba	180	160	400	460
Sc	15	15	15	15
V	110	105	110	115
Cr	300	280	280	300
Co	40	40	20	20
Ni	110	130	45	60
Cu	65	45	35	50
Ga	17	18	21	23
Zn	300	180	160	140
Pb	12	8	6	6
Th	1.0	1.0	1.0	1.0
U	1.5	0.5	0.5	2.0
Sb	3	3	3	2
Mo	4	4	4	4
W	125	96	71	61
Ta	5	4	4	4
La	12	11	13	17
Ce	22	20	24	31
Pr	3	2	3	4
Nd	12.5	10.0	12.5	14.5
Sm	2.5	3.0	2.5	1.5
Eu	1.5	1.0	1.5	1.5
Gd	4	4	4	4
Tb	0.5	0.5	0.5	0.5
Dy	3.5	3.0	4.0	4.0
Ho	0.5	0.5	0.5	0.5
Er	2	2	2	2
Tm	1	1	1	1
Yb	1	1	1	1
Lu	0.5	0.5	0.5	0.5

Basalt petrography and geochemistry

Even at the hand specimen scale it is evident that the basalt (which enclosed the fossilized wood) in the

Figure 27. Polarized light photomicrograph of basalt sample BCM-3 from Drill-hole 05469 from close to the entombed fossilized wood (Figure 12). The large (1.5 mm wide) grain in the top left corner is former olivine altered to chlorite and serpentine (green), goethite (brown) and iddingsite? (blue-green). Small (0.5–1 mm long) plagioclase laths (white) are scattered uniformly through the rock, but the clinopyroxene (probably augite) between the laths has been altered to chlorite with titanomagnetite grains (black) and iron oxide staining. (Approximately 60 times magnification.)

Figure 28. Polarized light photomicrograph of basalt sample BCW-2 from the large outcrop beside the waterhole in Crinum Creek (Figure 13.) Rounded equidimensional grains (1.5–2 mm wide) of altered olivine and lath-like crystals (1.5–2 mm long) of olivine are scattered between plagioclase laths (1–1.5 mm long) with intergranular clinopyroxene (augite?) altered to chlorite and small altered titanomagnetite grains. (Approximately 60 times magnification.)

drill core is more altered and/or weathered than the basalt from the outcrop beside Crinum Creek. This was verified by thin section examination (Figures 27 and 28). The basalt in the drill core does, in fact, come from the zone of weathering (Figure 3) where percolating oxidizing ground water readily alters minerals and rock chemistry by dissolving and removing various elements. On the other hand, the basalt outcrop beside Crinum Creek is expected to be relatively fresh because the fact that the basalt outcrops signifies it has survived weathering.

Very little trace of olivine is left in the basalt from the drill core. In thin section (Figure 27) all that is left of the olivine are the outlines of the former 1–1.5 mm wide grains, which have been altered to pale green chlorite, serpentine, and goethite. The serpentine is evident from the framework/window structure stained by brown goethite, and the residual smaller grains of bright blue-green iddingsite(?). It is hard to estimate, but the original proportion of olivine in the rock could have been at least 10%. The small (0.5–1 mm long) plagioclase laths, of which 40–45% of the rock consists, are still visible, but all the clinopyroxene (probably augite, and 35–40% of the rock) has been altered to chlorite and heavily stained with goethite and other iron oxides. Titanomagnetite (5–10%) would have made up the rest of what was probably a typical olivine basalt.

In contrast, some relatively unaltered olivine is visible in thin section in the basalt from the outcrop beside Crinum Creek (Figure 28). However, the sample of massive basalt form deeper within the flow is somewhat less altered than the sample of vesicular basalt from the near top of the flow. As well as rounded and equidimensional grains of altered olivine up to 1.5–2 mm wide, there are lath-like crystals of mostly fresh olivine up to 1.5–2 mm long, all recognized by their high birefringence and internal fractures. The rock consists of at least 10% olivine. The plagioclase laths are generally larger (1–1.5 mm long) in this basalt and make up about 45% of the rock, while the intergranular clinopyroxene (probably augite) is largely altered to chlorite and seems to be about 35% of the rock. There is very little iron oxide staining—only of the altered olivine grains and some of the chloritized clinopyroxene. However, the titanomagnetite (around 10% of the rock) has been altered to leucoxene and hematite(?). This rock is only slightly different in its mineralogical make-up and texture, but is still an olivine basalt similar to (but less than) that in the drill core.

The major and selected trace element analyses of some basalts are listed in Table 2. The loss on ignition, which is a measure of the content of H_2O and CO_2, (CO_2 from carbonates), in these basalts is moderate but consistent with the alteration and weathering (H_2O in chlorite, serpentite) observed in thin section. However, considering the amount of goethite/iron oxide staining in the basalt from the drill core, particularly, the Fe_20_3 (total Fe) content seems somewhat low and the Al_20_3 content correspondingly high, but this may reflect the composition of the predominant chlorite alteration. Otherwise, the MgO contents of the outcrop samples are reasonably consistent with the presence

in them of fresh olivine (particularly in the massive basalt from deeper in the flow), whereas the MgO content of the basalt in the drill core enclosing the fossilized wood is noticeably much lower, a result of the alteration of all the olivine. Furthermore, the TiO_2 contents of all the basalt samples are depleted compared with analyses of comparable basalts in the Springsure area south of Emerald (Joplin, 1963).

However, the major anomaly is the high SiO_2 contents of these olivine basalts, which would be expected to be in the 46–50% range, consistent with the related basalts of the Springsure area (LeMaitre et al., 1989). With SiO_2 contents of 54.5–55% (outcrop) and 60–61% (drill core), these basalts actually plot on the total alkalis (Na_2O+K_2O) versus SiO_2 (TAS) plot in the basaltic andesite and andesite fields respectively (Le Maitre et al., 1989) (Figure 29). On the other hand, whereas these major elements are highly mobile during alteration and weathering, many trace elements are relatively immobile and highly incompatible, and therefore, because they are retained once lavas crystallize, they can be used to discriminate original rock types even after alteration and weathering. Thus on the Zr/Ti versus Nb/Y discrimination diagram these olivine basalts correctly plot close together in the alkali basalt field (Pearce, 1996; Winchester & Floyd, 1977) (Figure 30). This would indicate then that Si was added during alteration and weathering and/or other major elements (Mg, Fe, Ca, Na, K, Mn) which are mobile were depleted relative to Si.

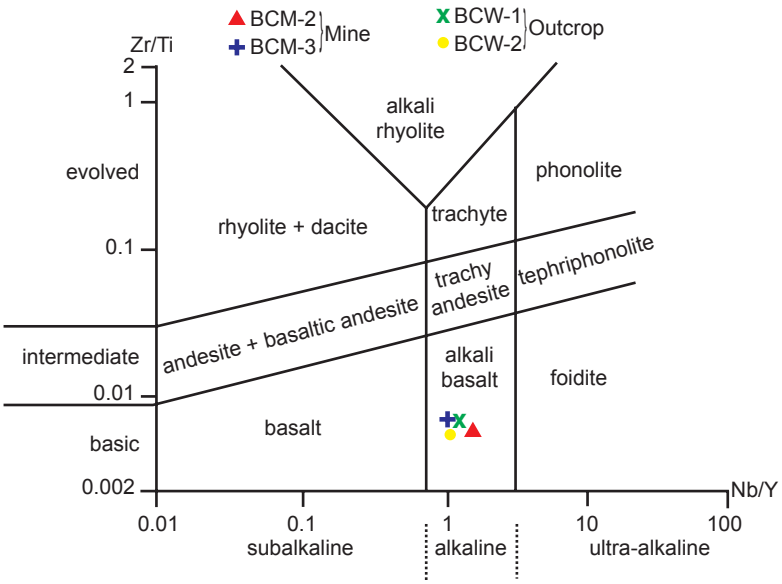

Figure 30. The Zr/Ti versus Nb/Y discrimination diagram for volcanic rocks and particularly basalts (after Pearce, 1996; Winchester & Floyd, 1977).

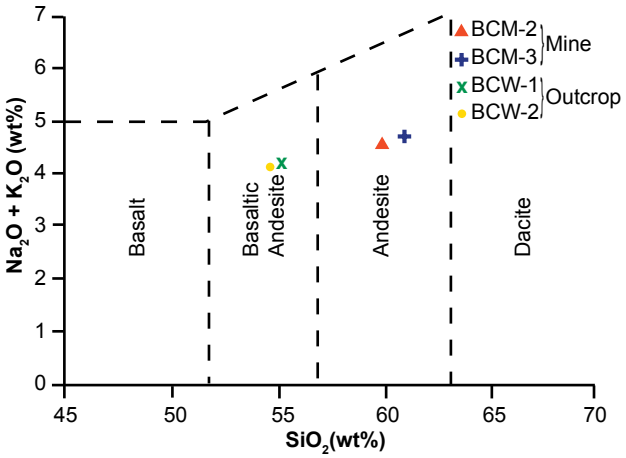

Figure 29. Total alkalis (Na_2O + K_2O) versus silica (SiO_2) or TAS diagram (after Le Maitre et al., 1989) for classification of volcanic rocks. The Crinum basalt samples plot in the basaltic andesite and andesite fields.

There are a number of normalized multi-element diagrams or incompatible element diagrams (spider diagrams) that are useful in geochemically characterizing basalts and for distinguishing their magma type and tectonic setting (Pearce, 1996; Rollinson, 1993). These Tertiary olivine basalts at Crinum are readily classified as within-plate, continental alkali basalts, and this is verified by

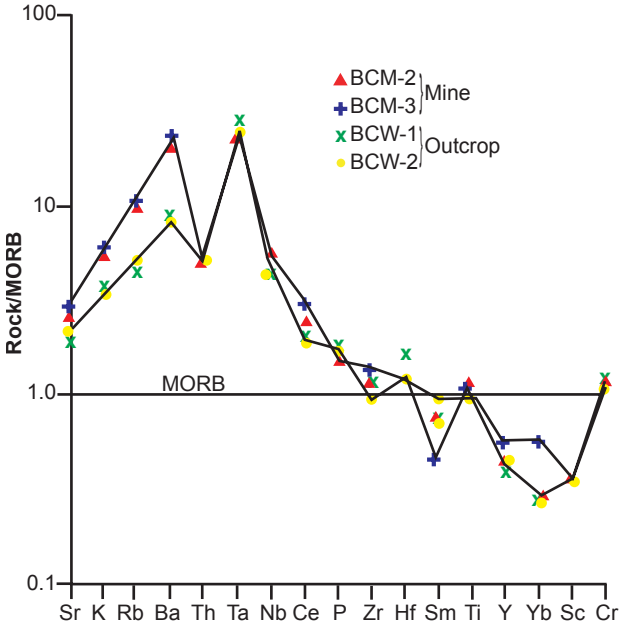

Figure 31. The MORB (mid-ocean ridge basalt)-normalized multi-element/incompatible element diagram (after Pearce, 1983) showing "spidergrams" for Crinum basalt samples BCM-3 and BCW-2. Normalizing values used are those of Pearce (1983, 1996).

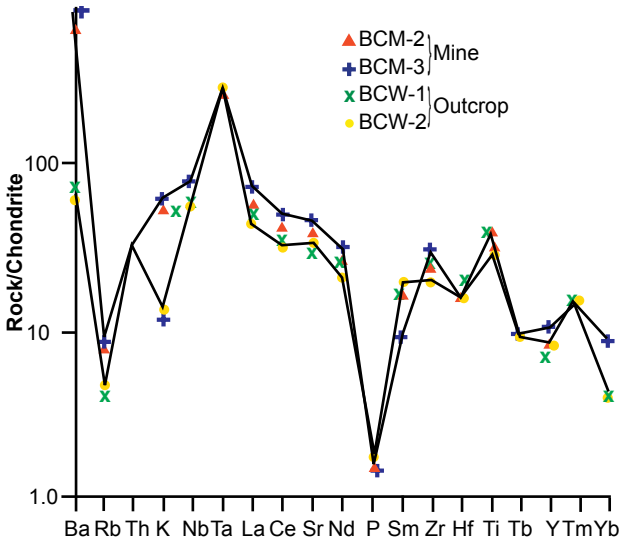

Figure 32. The chondrite (chondritic meteorite)-normalized multi-element/incompatible element diagram (Rollinson, 1993) showing "spidergrams" for Crinum basalt samples BCM-3 and BCW-2. Normalizing values used are those of Sun (1980) and Sun & McDonough (1989).

the steep negative slope and the matching shape of the "spidergrams" in the MORB-normalized multi-element/incompatible element diagram (Pearce, 1983; Rollinson, 1993; Saunders & Tarney, 1984; Sun, 1980; Weaver & Tarney, 1984) (Figure 31). Indeed, the pattern of trace element concentrations in this diagram has affinities to that of ocean island basalts, which therefore suggests a similar source. However, the "spidergrams" on the chondrite-normalized multi-element/incompatible element diagram (Figure 32) do not completely match that for ocean island basalts but are suggestive of additional lower continental crust influence, probably as contamination (Rollinson; Saunders & Tarney; Sun; Sun & McDonough; Weaver & Tarney). One glaring anomaly is the very low relative P content of these basalts, but the Rb, Th, and K are also lower than expected, which in the case of those elements could be explained by their mobility during alteration and weathering. On the other hand, the rare earth elements (REE) are regarded as amongst the least soluble trace elements and are relatively immobile during alteration and weathering (Rollinson), so the REE abundances in rocks produce characteristic "spidergrams" on chondrite-normalized REE diagrams. The REE "spidergrams" for these Crinum basalts are plotted in Figure 33 and are as expected for such alkali basalts—a negative slope due to light REE enrichment relative to heavy REE, and a positive Eu anomaly (Boynton, 1984; Rollinson, 1993). The low relative Sm in the basalt from the drill core is unexpected and may indicate some Sm loss, which like the apparent Rb, Th, and K losses could be significant for the respective radioisotopic systems.

Basalt K-Ar "dating"

The K-Ar "dating" results for the Crinum basalts are listed in Table 3. The calculated "model ages" range from 36.7±1.2Ma to 58.3±2.0Ma, which is an unacceptable outcome for analyses of two samples from the same lava flow intersected in the drill core. This problem of obtaining consistently acceptable "model ages" is highlighted by the fact that the same sample from the outcrop (BCW-2) submitted to both laboratories yielded "model ages" of 39.1±1.5Ma (Geochron) and 47.9±1.6Ma (AMDEL). Because the other sample from the outcrop (BCW-1) yielded a result between these two "model ages" it is tempting to assign an averaged "model age" of about 43.9Ma to this basalt. For the basalt in the drill core an averaged "model age" would be 47.5Ma, which would appear to be consistent with it being an older flow (because it is at the base of this Tertiary sequence).

However, when the fossilized wood was discovered at Crinum during excavation of the ventilation shaft the expected "age" of the basalt was suggested as only 30Ma (Anonymous, 1994; Chalmers, 1994), which would have been due to the published K-Ar whole-rock "model ages" of 27.9Ma and 32.7Ma for comparable olivine basalt samples from outcrops of the same Tertiary basalt flows south of Emerald towards Springsure (Webb & McDougall, 1967). It was argued there that this spread of "ages" most probably reflected varying degrees of Ar leakage from the flows, which were suggested to be all at least 33Ma, due to the alteration of the 5–10% intersertal cryptocrystalline material in the basalt (and in some instances to the alteration of the olivine and/or the plagioclase) (Webb & McDougall). Nevertheless, because the alteration of those basalts was presumed to be deuteric and thus contemporaneous with consolidation of the lavas, and

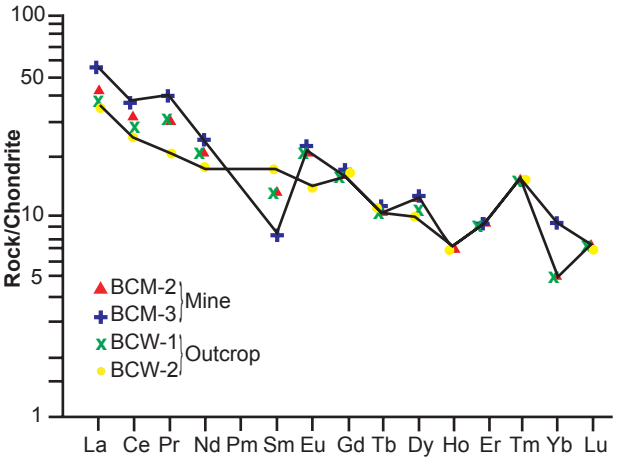

Figure 33. The chondrite (chondritic meteorite)-normalized REE (rare earth element) diagram (Rollinson, 1993) showing "spidergrams" for Crinum basalt samples BCM-3 and BCW-2. Normalizing values used are those of Boynton (1984).

Table 3. Potassium-argon (K-Ar) isotopic analyses and age determinations on the Crinum basalts.

Sample	Lab Code	K_2O (wt%)	^{40}K (ppm)	$^{40}Ar^*$ (ppm) $\times 10^{-3}$	$^{40}Ar^*$ (%)	Total ^{40}Ar (ppm)	$\frac{^{40}Ar^*}{\text{Total } ^{40}Ar}$	$\frac{^{40}Ar}{^{36}Ar}$	^{36}Ar (ppm) $\times 10^{-5}$	$\frac{^{40}Ar^*}{^{36}Ar}$	$\frac{^{40}K}{^{36}Ar}$ ($\times 10^3$)	Model Age (Ma)	Uncertainty (Ma) (1σ)
BCW-1 (outcrop)	Amdel	0.548	0.654	1.725	4.40	0.039205	0.044	—	—	—	—	44.9	1.1
		0.547	0.653	1.724	4.40	0.039182	0.044	—	—	—	—	44.8	1.1
BCW-2 (outcrop)	Amdel	0.491	0.586	1.661	4.40	0.037750	0.044	—	—	—	—	47.9	1.6
		0.496	0.592										
BCW-2 (outcrop)	Geochron (R-11800)	0.529	0.631	1.448	5.70	0.025404	0.057	314	8.09	7.802	17.898	39.1	1.5
BCM-2 (drill core)	Geochron (R-11798)	0.862	1.028	3.537	4.70	0.075255	0.047	311	24.19	4.249	14.617	58.3	2.0
BCM-3 (drill core)	Geochron (R-11799)	0.870	1.038	2.234	3.80	0.053789	0.038	307.5	17.49	7.687	11.685	36.7	1.2

Notes: (1) The mean K values were used in the age calculations
(2) $^{40}Ar^*$ denotes radiogenic ^{40}Ar
(3) Ages in Ma with error limits given for the analytical uncertainty at one standard deviation

Constants: $^{40}K = 0.01167$ atom%, $^{40}K/K = 1.193 \times 10^{-4}$ g/g
$\lambda_\beta = 4.962 \times 10^{-10}$/year, $\lambda_\varepsilon = 0.581 \times 10^{-10}$/year

because of the general agreement of these "dates" with those K-Ar "ages" obtained from sanidine crystals in cogenetic rhyolites, it was concluded that there must have been no appreciable leakage of radiogenic Ar ($^{40}Ar^*$) from the whole-rock samples, the alteration products (in most cases) having retained almost all $^{40}Ar^*$ despite the fine grain size.

Thus it is very likely the K-Ar "model ages" obtained for the Crinum basalts (Table 3) are far too high. Both laboratories reported an abnormally high atmospheric Ar component in the analyses so that the ratios of $^{40}Ar^*$ to total ^{40}Ar were quite low (Reesman, 1997; Webb, 1995), and this was suggested as possibly due to the goethite and other fine-grained alteration products, including some glassy mesostasis. Yet if the experience with the comparable olivine basalts south of Emerald is valid, then there has probably been no appreciable $^{40}Ar^*$ leakage from the alteration products in these Crinum basalts, so the explanation for these unacceptable older "model ages" must lie elsewhere.

One possibility is loss of K during weathering, but this is discounted by the fact that there is more K in the more altered basalt in the drill core than in the less altered outcrop basalt. If this difference is due to the alteration process, then K may have in fact been thereby added to the basalt in the drill core. On the other hand, because the two basalt outcrop samples have approximately the same K concentration, while the two drill core basalt samples have higher, and identical, K concentrations (Table 3), the difference may reflect different primary K concentrations in the basalts when extruded.

Another possibility is excess $^{40}Ar^*$ present initially in the lavas when extruded, inherited from the upper mantle source area of the basaltic magma, which has been demonstrated to be a persistent and widespread problem for the K-Ar "dating" of volcanics, and crustal rocks generally (Snelling, 1998). It is very significant, therefore, that even though both laboratories reported extreme levels of atmospheric Ar contamination, Geochron also reported with their analyses $^{40}Ar/^{36}Ar$ ratios much higher than the atmospheric $^{40}Ar/^{36}Ar$ ratio of 295.5 (Reesman, 1997) (Table 3). This implies excess $^{40}Ar^*$ in these basalts, which was not derived from in situ decay of parent ^{40}K. Thus, because in the standard K-Ar "model age" calculations used by the laboratories all the analyzed $^{40}Ar^*$ in the samples was assumed to have been derived by in situ ^{40}K decay, when in fact some excess $^{40}Ar^*$ is present, then the resultant "model ages" are probably too high. In any case, it is clear from close examination of the analytical results in Table 3 that the variations in $^{40}Ar^*$ between the samples beyond proportionality with ^{40}K are primarily responsible for the variation sin the K-Ar "model ages." What the "correct age" is for the Crinum basalts remains unclear, as does the validity of K-Ar "dating." There was also too much scatter and not enough spread in the data to determine any isochron "ages."

Basalt Sr-Nd-Pb Isotopic Geochemistry

The results from the Rb-Sr, Sm-Nd, and Pb-Pb isotopic analyses of the same four basalt samples are listed in Tables 4, 5, and 6 respectively. These radioisotopic systems are, of course, regularly used for "dating" of rocks and minerals, particularly with the isochron method. However, because of the long half-lives of these parent radioisotopes and the relatively young expected "age" of these Tertiary Crinum basalts (about 30–33 Ma), these radioisotopic systems are usually unable to provide statistically meaningful results. Moreover, there is insufficient spread in the data, particularly the $^{87}Sr/^{86}Sr$ and $^{143}Nd/^{144}Nd$ ratios (Tables 4 and 5), to produce isochrons with slopes sufficient for "age" calculations. Indeed, both the Rb-Sr and Sm-Nd data when plotted yield isochrons which are virtually horizontal. Furthermore, the resultant isochrons do not fit the data well and thus yield poor statistics, unacceptably large MSWDs, and

Table 4. Rubidium-strontium (Rb-Sr) isotopic analyses of the Crinum basalts.

Sample	Rb (ppm)	^{87}Rb (nm/g)	Sr (ppm)	^{86}Sr (nm/g)	^{87}Sr/^{86}Sr	^{87}Sr/^{86}Sr *
BCM-2	21.20	68.825	340.67	383.64	0.17940	0.704204±19
BCM-3	24.94	80.966	366.98	413.27	0.19592	0.704269±20
BCW-1	13.66	44.365	306.20	344.83	0.12866	0.704160±21
BCW-2	13.50	43.900	307.48	346.26	0.12678	0.704227±25

Notes: (1) *Measured, present-day ^{87}Sr/^{86}Sr ratios (±2σ), normalized to ^{86}Sr/^{88}Sr = 0.1194.
(2) The ^{87}Sr/^{86}Sr value for the N.B.S. Sr isotope standard (SRM 987) run with these samples was 0.170207±26 (±2σ).

Table 5. Samarium-neodymium (Sm-Nd) isotopic analyses of the Crinum basalts.

Sample	Sm (ppm)	^{147}Sm (nm/g)	Nd (ppm)	^{144}Nd (nm/g)	^{147}Sm/^{144}Nd	^{143}Nd/^{144}Nd *	$\varepsilon_{Nd}(t_0)$
BCM-2	3.152	3.144	5.329	8.789	0.35770	0.512800±13	+2.380
BCM-3	3.181	3.173	12.269	20.236	0.15680	0.512796±9	+2.302
BCW-1	1.523	1.519	5.180	8.544	0.17780	0.512794±11	+2.263
BCW-2	1.3379	1.3343	10.109	16.673	0.08003	0.512795±13	+2.282

Notes: (1) *Measured, present-day ^{143}Nd/^{144}Nd ratios, normalized to ^{146}Nd/^{144}Nd = 0.7219.
(2) $\varepsilon_{Nd}(t_0)$ refers to the present-day, calculated relative to a BCR-1 value of 0.512678.

Table 6. Lead-lead (Pb-Pb) isotopic analyses of the Crinum basalts.

Sample	^{206}Pb/^{204}Pb	^{207}Pb/^{204}Pb	^{208}Pb/^{204}Pb
BCM-2	18.623	15.638	38.661
BCM-3	18.647	15.650	38.705
BCW-1	18.556	15.571	38.485
BCW-2	18.741	15.736	38.893

Note: All isotopic ratios were corrected for mass fractionation using a ^{207}Pb-^{204}Pb double spike (after Woodhead et al., 1995).

2σ errors which are larger than the "ages" calculated from the isochrons. "Model age" calculations also produce useless results.

Where these isotopes prove useful, however, is in geochemical "fingerprinting" of the mantle source area of the basalt magma. For example, when young oceanic basalts are plotted on an Nd-Sr isotope correlation diagram (Figure 34) they fall within a narrow sloping linear band across the diagram referred to as the "mantle array" (DePaolo & Wasserburg, 1979; Dickin, 1995; Dosso & Murthey, 1980). The Crinum basalts also plot within this "mantle array," which has been attributed to a chondritic lower mantle source contaminated by mixing with melts from a depleted MORB (mid-ocean ridge basalt) source during ascent. However, on both the Nd-Sr isotope correlation diagram (Figure 34) and the ε_{Nd}-Sr isotope correlation diagram, (Figure 35) the Crinum basalts plot very close to the Bulk Earth mantle reservoir, which is regarded as the chemical composition of the earth without the core (all of the earth made up of only silicate minerals). The Crinum basalts also plot close to other continental basalts on the ε_{Nd}-Sr isotope correlation diagram (Figure 35) and thus show no signs of crustal radiogenic Sr contamination. Furthermore, when Nd-Sr isotopic compositions of oceanic volcanics are plotted, there can be evidence of a second array different from the main mantle array (Figure 36). This shallow mixing line has been attributed to sediment recycling—the addition of subducted sediments with a crustal radiogenic Sr component due to the recycling of oceanic crust (Dickin, 1995; Hofmann & White, 1982). However, the Crinum basalts plot in the main mantle array, which can also be interpreted as a mixing

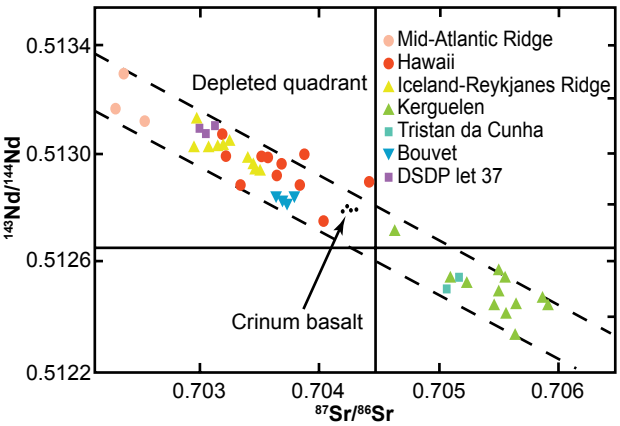

Figure 34. Nd-Sr isotope correlation diagram for oceanic volcanic rocks showing the linear correlation referred to as the "mantle array" (after DePaolo & Wasserburg, 1979; Dosso & Murthey, 1980). The Crinum basalt samples plot in the "mantle array" close to the "Bulk Earth" composition, though slightly depleted.

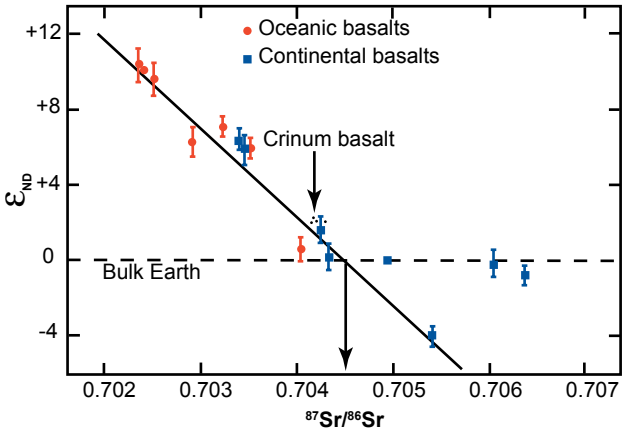

Figure 35. ε_{ND}/Sr isotope correlation diagram for ocean floor ocean island and continental basalts (after DePaolo & Wasserburg, 1976). The Crinum basalt samples plot with other continental basalts along a linear correlation and near the "Bulk Earth" composition, and no crustal radiogenic Sr contamination is evident in them, unlike other continental basalts which plot to the right of the linear correlation.

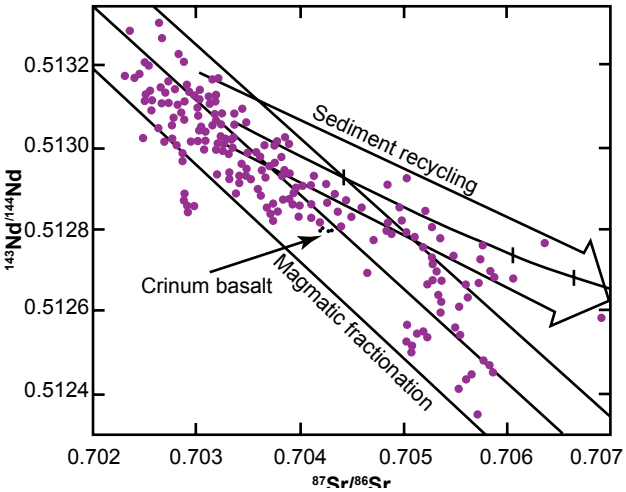

Figure 36. Plot of Nd-Sr isotope compositions of oceanic volcanic rocks showing two arrays—recycling of magmatically fractionated material and sediment recycling [after *Hofmann and White*, 1982.] The Crinum basalt samples lot near the center line of the magmatic fractionation array, and show no evidence of any contamination due to sediment recycling.

line attributed to the recycling of magmatically fractionated material such as ancient oceanic crust.

The Pb isotopic geochemistry of these Crinum basalts, on the other hand, is enigmatic. When the Pb isotopic compositions of young ocean island basalts (OIBs) are plotted on a ^{207}Pb-^{206}Pb "isochron" diagram they define a series of linear arrays to the right of the geochron (Dickin, 1995; Sun, 1980) (Figure 37). The geochron is the isochron connecting the assumed primordial Pb isotopic composition (that of the troilite from the Canyon Diablo meteorite) with the Pb isotopic compositions of iron and stony meteorites and terrestrial pelagic sediment (regarded as a Bulk Earth composition), which defines the supposed 4.57 Ga age of the earth (Patterson, 1956). The distribution of these OIB Pb-Pb arrays to the right of the geochron presents a problem for the understanding of evolutionary models of Pb isotopes in the earth as a whole, particularly as the slopes of these OIB arrays correspond to apparent Pb-Pb "ages" of between 1.0 and 2.5 Ga (Dickin). Intriguingly, the Pb isotopic compositions of the Crinum basalts also define a linear array to the right of the geochron, with its slope corresponding to an apparent Pb-Pb "age" of 5.07±0.27 Ga (though the MSWD is too large for this "result" to have any statistical significance).

These OIB linear Pb-Pb isotopic arrays have been interpreted in three principal ways—as resulting from discrete mantle differentiation events (Chase, 1981); as the products of two-component mixing processes (Sun, Tatsumoto, & Schilling, 1975); or resulting from continuous evolution of reservoirs with changing μ ($^{238}U/^{204}Pb$) values (Dupre & Allegre, 1980).

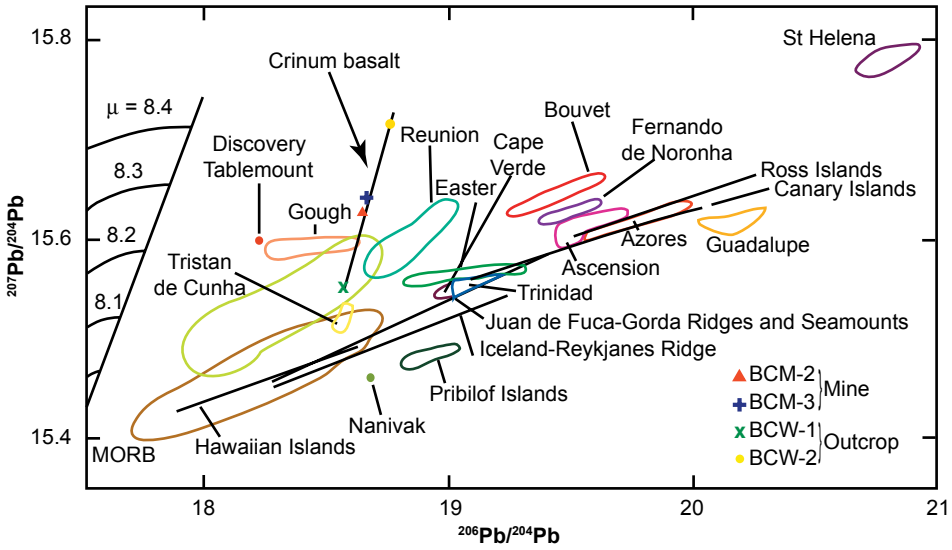

Figure 37. Pb-Pb "isochron" diagram showing linear arrays of data defined by ocean island basalts [after *Sun*, 1980]. The geochron was defined by *Patterson* [1956]. The Crinum basalt samples define a linear array, the slope of which corresponds to an apparent Pb-Pb "age" of 5.07±0.27 Ga.

The steep slope of the linear array produced by the Crinum basalts clearly reflects different μ values. The two drill-core samples of the basalt plot close together with a similar μ value, but the two basalt outcrop samples have widely divergent μ values, even though they probably represent the same flow. This difference cannot be the result of alteration of weathering, because the outcrop samples have suffered very little alteration and weathering compared to the drill-core samples. Besides, Pb isotopes have been shown to be unperturbed by alteration and weathering (Rosholt & Bartel, 1969), so the difference must be a primary feature. Furthermore, this linear array cannot be the product of a discrete mantle differentiation event because its apparent Pb-Pb "age" is older than the earth itself, unless the Pb isotopes are not recording "ages." On the other hand, two component mixing is discounted by the Nd-Sr isotopic correlations which indicate a fairly homogeneous mantle source and no crustal radiogenic Sr contamination, that is, no mixing of a crustal component with the mantle reservoir. It is thus concluded that the Pb-Pb isotopic linear array of these Tertiary Crinum basalts is a primary geochemical feature of their otherwise homogeneous mantle source and has no "age" significance.

Discussion

The identification of the fossilized wood as probably belonging to the genus *Melaleuca* and of the fossilized leaf as probably belonging to the family *Lauraceae* is consistent. Both living types are found in Australia today in wet environments, where a variety of trees grow adjacent to one another. An example of a *Melaleuca* today is the teatree, while *Lauraceae* grow today in wet rainforest, such as that on the Lamington Plateau near the Queensland-New South Wales border, inland behind the Gold Coast. Thus this fossilized wood and the leaf imprint suggest a reasonably wet and humid environment in the Crinum area in the recent past. This is in marked contrast to the climate and environment in the area today. The landscape is well-drained and dry for much of the year, and dominated by *Eucalyptus*, with *Bauhinia* and *Casuarina* trees growing along Crinum Creek. Most of the rain falls in the summer months from tropic/sub-tropical storms which pass inland. *Melaleuca* and *Lauraceae* definitely do not grow in the Crinum area today.

However, *Lauraceae* leaf fossils are common in localised early Tertiary (Eocene) deposits scattered across Australia, from Anglesea on the Victorian coast west of Melbourne, to Moranbah in central Queensland, the Lake Eyre area in northern South Australia (which is desolate and arid today), and West Dale in the south-west of Western Australia (Christophel, 1994). An analogous extant flora to that found fossilized at Anglesea is that at Noah Creek on Queensland's northern tropical coast. The best documented of these fossil floras is at Nerriga in New South Wales (140 km east of Canberra), where fossilized *Lauraceae* leaves have generally been mummified, in contrast to the leaf impression at Crinum (Hill, 1986). At Moranbah in the northern Bowen Basin, about 145 km north of Crinum, fossilized *Lauraceae* leaves occur in clay capped by basalt, dated radiometrically and by pollen accompanying the fossilized leaves as of Eocene "age" (Christophel, 1994). The 43.9 Ma and 47.5 Ma K-Ar "model ages" obtained on the Crinum basalts are thus consistent with the enclosed *Lauraceae* leaf impression and *Melaleuca* fossilized wood at Crinum being also of Eocene age.

On the other hand, as already noted, due to the well-established and published K-Ar "model ages" of 27.9 Ma and 32.7 Ma for comparable olivine basalt samples from outcrops of the same Tertiary basalt flows south of Emerald (Webb & McDougall, 1967), it is very likely that these K-Ar "model ages" for the Crinum basalts are far too high. Excess $^{40}Ar^{*}$, not derived from in situ decay of parent ^{40}K and therefore present in the basalts initially, inherited from the magma source area, is suggested as the culprit. If these conclusions are correct, then the Crinum basalts and the enclosed fossilized wood and leaf impression would be early Oligocene in age (in conventional terms), a little younger than the Moranbah fossil flora.

The chronological framework for regional volcanism also puts constraints on the "age" of the Crinum basalts (Grimes & Withnall, 1995; Sutherland, 1978). When the K-Ar "model ages" of all the volcanic rocks of Eastern Australia and their geographical locations are plotted there appears to be a consistent pattern of sub-parallel linear trends along which the volcanism has occurred at progressively younger "ages" in a south-south-west direction (Sutherland, 1978, 1985). Thus there is a trend line of volcanism running from Cape Hillsborough on the central Queensland coast (33 Ma) south-south-west through Nebo in the northernmost Bowen Basin (32 Ma), North Clermont (31 Ma) and South Clermont (28–29 Ma) in the central Bowen Basin, to the Springsure area (27 Ma) south of Emerald, and it appears this trend line continues south-south-west through younger centres of volcanism in western New South Wales and central Victoria. The Crinum basalts appear by proximity and field relations to be related to, and part of, the volcanic centres and lava fields of South Clermont and Springsure (Grimes & Withnall, 1995; Webb & McDougall, 1967) which would make their "age" around 28 Ma, and the fossilized wood and leaf middle Oligocene (in conventional terms).

The explanation given for this, and the other sub-parallel, south-south-westerly younging trends of volcanism, is the drift of the Australian plate over as many as seven stationary hotspots/mantle plumes producing hotspot trails similar to the classical hotspot trail along the chain of Hawaiian Islands (Sutherland, 1985; Wellman, 1983). The direction of the younging trend and the rate of plate drift is said to be determined by the sea-floor spreading in the Southern Ocean and Coral Sea. Plate motion in the Tertiary-Recent has essentially been northwards as Australia separated from Antarctica, the drift rate being calculated from radioisotopic dating of this hotspot volcanism and ocean floor basalts related to sea-floor spreading. On the other hand, the hotspots/mantle plumes are regarded as being related to magma sources formed at the sea-floor spreading rift in the Coral Sea due to thermal anomalies in the mantle. The location of the volcanism itself at particular sites is considered as being related to structural weaknesses, including basin margins (relevant to the western margin of the Bowen Basin in the Clermont area), faults and major lineaments (perhaps linked to transform faults in the Tasman Sea related to sea-floor spreading and plate motion).

The mineralogy, the major, trace and rare earth element geochemistry, and the Sr-Nd-Pb isotopic geochemistry are all consistent with these basalts being hotspot/mantle-plume-derived, within-plate, continental alkali basalts, as indicated also by the tectonic setting. The isotopic geochemistry suggests a mantle source for the Crinum basalts without any recycled crustal component and the tectonic setting confirms this. The hotspot/mantle plume source developed beneath oceanic crust in a sea-floor spreading setting remote from the influence of terrigenous sediments and their crustal isotopic signatures. It has been suggested that as much as 15% or more partial melting of upper mantle rock must have occurred to supply these alkali basalts (Sutherland, 1985), resulting in recycling of magmatically fractionated material as implied by their isotopic geochemistry. Such partial melting may well have been triggered by upward flow of a volatile-rich fluid and accompanying heat from deeper in the mantle (Middlemost, 1985), the volatiles including excess $^{40}Ar^{*}$.

All the field evidence indicates that the wood was fossilized as a result of being entombed in the lowermost of these Tertiary alkali basalt flows at Crinum. The trees were apparently rooted in the Permian siltstone at the Tertiary land surface over which the lava flowed. Without doubt, the wood must be the same age as the basalt which entombed it. However, an apparent conflict arises because the fossilized wood contains radiocarbon which yields a ^{14}C "age" of around 37,500 years BP, whereas the basalt has been labelled "Tertiary" with a K-Ar "age" of 47.5 Ma (the basalt in the drill core enclosing the fossilized wood), though this latter "result" should probably be around 30 Ma due to the inclusion of excess $^{40}Ar^{*}$ in the basalt. The reliability of K-Ar "dating" is, of course, questioned, and the true age of the basalt based on radioisotopic dating remains unclear. The "acceptable" 30 Ma "age" is simply a product of correlation with other K-Ar "ages" for comparable nearby basalts and the regional chronological framework (Grimes & Withnall, 1995; Webb & McDougall, 1967), all of which is based on uniformitarian assumptions.

Quite obviously, the radiocarbon "age" for the fossilized wood is drastically short of the 30 Ma or more for the basalt, when they should both be the same "age." Of course, uniformitarian geologists would probably not have even tested this fossilized wood for radiocarbon, because they would not expect any to be in it. No detectable ^{14}C should have remained in the fossilized wood if it is older than about 55,000 years (10 half-lives of 5,570 years), and the fossilized wood is supposedly at least 30 Ma, the "age" of the basalt. Because measurable radiocarbon has been unequivocally demonstrated to be in this fossilized wood, uniformitarian geologists would assume this to be due somehow to contamination. But such a criticism is totally unjustified for the reasons already discussed, including the percent modem carbon in the samples and the extreme uniformity and consistency of the $\delta^{13}C_{PDB}$ values. Thus the radiocarbon in the fossilized wood may be a better guide to the "age" of the basalt than the K-Ar "dating."

The Results in the Context of the Biblical Flood Model

In the Creation/Flood framework for earth history, the observation that these trees were probably growing on a land surface that in relative terms existed very late in earth history after many fossil-bearing strata (the Permian marine fossiliferous strata and coal seams) had been catastrophically laid down would make these trees post-Flood. Furthermore, the identification of the fossilized wood as probably *Melaleuca* and the leaf imprint as *Lauraceae* implies a wet environment (perhaps rainforest) where today it is relatively dry (before clearing, probably dry schlerophyll). This is consistent with this land surface and the trees being immediate post-Flood, when the climate was still drying out after the Flood. Thus the basalt lava flowed across this post-Flood land surface, and so, like the fossilized wood it entombed, it is less than 4,500 years old. In this framework, the radiocarbon in the fossilized wood has not provided the true age of the fossilized wood and the enclosing

basalt, but it clearly demonstrates that they cannot be millions of years old.

An excessively large finite radiocarbon "age" for this fossilized wood is neither inconsistent nor unexpected within the Creation/Flood framework of earth history. Engulfed by the basalt lava flow less than 4,500 years ago, this Crinum fossilized wood contains less than the expected amount of about 4,500 years worth of radiocarbon. During the Flood and the immediate post-Flood periods, the earth's stronger, but fluctuating, magnetic field would have more effectively shielded the earth from the incoming cosmic ray flux, which in turn would have resulted in a lower radiocarbon production rate (Humphreys, 1986). Thus there would have been much less radiocarbon in the atmosphere back then, and much less in the vegetation. Since the laboratories calculated the ^{14}C "ages" for the fossilized wood samples based on the assumption that the level of atmospheric radiocarbon in the past has been roughly the same as the level in 1950, the resultant radiocarbon "ages" are very much greater than the true ages.

Furthermore, the Flood also buried a lot of carbon. Thus the stable ^{12}C would not have been totally replaced in the biosphere after the Flood, whereas ^{14}C would have been regenerated in the atmosphere (from cosmic ray bombardment of nitrogen) and then in the biosphere. So the $^{14}C/^{12}C$ ratios in the pre-Flood organic materials (that is, organic materials that grew before the Flood but were buried during the Flood) and in immediate post-Flood organic materials (such as this Crinum fossilized wood), would have been much higher than today's $^{14}C/^{12}C$ ratio. Using today's ratio for calculating radiocarbon dates thus provides too high a calibration and yields inflated "ages."

Finally, the tectonic setting and origin of the Crinum basalt is not inconsistent within the Creation/Flood model of earth history. Given that plate tectonics occurred catastrophically during the Flood, with meters per second rates of plate movements initiated by thermal runaway subduction connected to sea-floor spreading by mantle-wide convective flow (Austin et al., 1994; Baumgardner, 1994a; 1994b), it is to be expected that plate movements slowed dramatically during the closing phase of the Flood but continued, finally decelerating to today's rates some years after the Flood. Thus the final stages of movement of the Australian plate into its current position could have occurred in the immediate post-Flood period. If the Flood/post-Flood boundary were to be placed at the Cretaceous/Tertiary boundary (Austin et al.) or somewhere soon thereafter in the early Tertiary, then by the early Oligocene (the conventional age of the Crinum basalt), trees would have again been growing on a wet but drying out, post-Flood landscape in the Crinum area. With the Australian plate also drifting northwards over a stationary hotspot/mantle plume, which was generated by residual convective volatile-rich fluid flow from deeper in the mantle, a structural weakness in the crust allowed magma from the partial melting of the upper mantle, to erupt as outpourings of the basalt lavas that engulfed trees and other vegetation in their path.

Conclusions

The fossilized wood found entombed in a Tertiary basalt flow during excavation of the upcast ventilation shaft at the Crinum Colliery in central Queensland was identified as probably *Melaleuca* and yielded a radiocarbon "age" of about 37,500 years BP. A leaf imprint found in the basalt was identified as probably *Lauraceae,* which like *Melaleuca* suggests a wetter environment than in the Crinum area today. The $\delta^{13}C_{PDB}$ values measured in the wood were uniform, averaging –25.69‰, consistent with the organic carbon in the fossilized wood being that of terrestrial plants. Thus the measured radiocarbon pertains to organic carbon remaining in the fossilized wood, and is not due to any contamination.

The basalt which entombed the fossilized wood, while showing alteration due to weathering, is an olivine-bearing alkali basalt. The basalt's incompatible trace and rare earth element geochemistry though is unaffected by weathering and is characteristic of within-plate continental alkali basalts, in this case with some affinities to ocean island basalts consistent with a mantle source. The basalt yielded conventional K-Ar "model ages" ranging from 36.7±1.2 Ma to 58.3±2.0 Ma. The averaged "model age" of 47.5 Ma was excessively old compared to the expected "age" of around 30 Ma, based on published K-Ar "model ages" of 27.9 Ma and 32.7 Ma for comparable basalts to the south of Crinum which are believed to be contemporaneous. Available evidence indicates the excessively old "ages" are due to excess $^{40}Ar^*$ in the basalt which was not derived from in situ decay of parent ^{40}K but inherited by the lava from its source. The Nd-Sr isotope geochemistry of the basalt is consistent with a homogeneous mantle source potentially involving the recycling of magmatically fractionated material such as older oceanic crust, but with no crustal radiogenic Sr contamination. The basalt also yields a Pb-Pb isotopic linear array with a slope corresponding to an apparent Pb-Pb "age" of 5.07±0.27 Ga (but with poor statistics), which is only significant as a primary geochemical feature of its mantle source. In its tectonic setting, this basalt was erupted due to hotspot/mantle plume volcanism as the Australian plate moved northwards.

All the Crinum observations and data are best explained within the Creation/Flood model of earth

history. The trees were growing in the immediate post-Flood period on a landscape that was drying out. After catastrophic plate movements during the Flood, the decelerating Australian plate drifted over a hotspot/mantle plume which produced outpourings of basalt lavas that engulfed the trees. The presence of the radiocarbon in the fossilized wood demonstrates that the enclosing basalt cannot be millions of years old and that the radioisotopic "dating" is grossly in error. While not providing the true age, the excessive radiocarbon "age" is consistent with a stronger magnetic field and changes in atmospheric ^{12}C levels around the earth during and immediately after the Flood.

Acknowledgments

This study would not have been possible without the co-operation and help of Greg Chalmers, then Chief Project Engineer for the Crinum Mine Project of BHP Australia Coal Pty. Ltd. Greg supplied the fossilized wood samples, the relevant drill cores, and copies of geological plans and sections, and hosted a visit to the Crinum Colliery. Acknowledgment is given and thanks extended. Answers in Genesis through the donations of its supporters kindly funded all the geochemical and isotopic analyses. The expertise and help of Dr. Geoff Downes of the CSIRO. Division of Forestry and Forest Products is also gratefully acknowledged.

References

Anonymous (December 1993–January 1994). Rare find unearthed at Crinum. *BHP Australia Coal Newsline,* 1.

Austin, S.A., Baumgardner, J.R., Humphreys, D.R., Snelling, A.A., Vardiman, L., & Wise, K.P. (1994). Catastrophic plate tectonics: A global Flood model of earth history. In R.E. Walsh (Ed.), *Proceedings of the third international conference on creationism (*pp.609–621). Pittsburgh, Pennsylvania: Creation Science Fellowship.

Baumgardner, J.R. (1994a). Computer modelling of the large-scale tectonics associated with the Genesis Flood. In R.E. Walsh (Ed.), *Proceedings of the third international conference on creationism (*pp.49–62). Pittsburgh, Pennsylvania: Creation Science Fellowship.

Baumgardner, J.R. (1994b). Runaway subduction as the driving mechanism for the Genesis Flood. In R.E. Walsh (Ed.), *Proceedings of the third international conference on creationism (*pp.63–75). Pittsburgh, Pennsylvania: Creation Science Fellowship.

Bird, M.I., Ayliffe, L.K., Fifield, L.K., Turney, C.S.M., Cresswell, R.G., Barrows, T.T., & David, B. (1999). Radiocarbon dating of "old" charcoal using a wet oxidation, stepped-combustion procedure. *Radiocarbon, 41*, 127–140.

Boynton, W.V. (1984). Geochemistry of the rare earth elements: Meteorite studies. In P. Henderson (Ed.), *Rare earth element geochemistry (*pp.63–114). Amsterdam: Elsevier.

Chalmers, G.B. (1994). Letter dated April 27, 1994 written to Dr. Geoff Downes of the CSIRO Division of Forestry and Forest Products. (Greg Chalmers was then the Chief Project Engineer for the Crinum Mine Project, BHP Australia Coal Pty. Ltd.).

Chalmers, G.B. (1994). Personal communications with Dr. Andrew A. Snelling during mine visit on August 31, 1994. (Greg Chalmers was then the Chief Project Engineer for the Crinum Mine Project, BHP Australia Coal Pty. Ltd.).

Chase, C.G. (1981). Oceanic island Pb: Two-stage histories and mantle evolution. *Earth and Planetary Science Letters, 52*, 277–284.

Christophel, D.C. (1994). The early Tertiary macrofloras of continental Australia. In R.S. Hill (Ed.), *History of the Australian vegetation: Cretaceous to recent (*chap.11, pp.262–275). Cambridge, England: Cambridge University Press.

DePaolo, D.J. & Wasserburg, G.J. (1976). Inferences about magma sources and mantle structure from variations of $^{143}Nd^{144}Nd$. *Geophysical Research Letters, 3*, 743–746.

DePaolo, D.J. & Wasserburg, G.J. (1979). Petrogenetic mixing models and Nd-Sr isotopic patterns. *Geochimica et Cosmochimica Acta, 43*, 615–627.

Devey, D.M. (1995). Gordonstone Mine. In I.L. Follington, J.W. Beetson, & L.H. Hamilton (Eds.), *Proceedings of the Bowen Basin symposium 1995 (*pp.299–301). Geological Society of Australia Coal Geology Group.

Dickin, A.P. (1995). *Radiogenic isotope geology.* Cambridge, England: Cambridge University Press.

Dosso, L. & Murthey, V.R. (1980). A Nd isotope study of the Kerguelen islands: Inferences on enriched oceanic mantle sources. *Earth and Planetary Science Letters, 48*, 268–276.

Dupre, B. & Allegre C.J. (1980). Pb-Sr-Nd isotopic correlation and the chemistry of the North Atlantic mantle. *Nature, 286*, 17–22.

Falkner, A. (1993). Sedimentological studies in the German Creek Coal Measures and their relevance to longwall mining. In J.W. Beetson (Ed.), *New developments in coal geology (a symposium) (*pp.143–148). Brisbane: Geological Society of Australia Coal Geology Group.

Fielding, C.R., Stephens, C.J., Kassan, J., & Holcombe, R.J. (1995). Revised palaeogeographic maps for the Bowen Basin, central Queensland. In I.L. Follington, J.E. Beetson, & L.H. Hamilton (Eds.), *Proceedings of the Bowen Basin symposium 1995 (*pp.7–15). Geological Society of Australia Coal Geology Group.

Grimes, K.G. & Withnall, I.W. (1995). Cainozoic geology of the Anakie-Rubyvale area. In I.W. Withnall (Ed.), *1995 Field Conference Clermont-Anakie Area (*pp.64–69). Brisbane: Geological Society of Australia, Queensland Division.

Hedges, R. (1998). Letter dated January 22, 1998 written to Mr. Jack Lewis of Isleham, Ely, England. (Professor Hedges has been the Director of the Radiocarbon Unit, Oxford University, England.)

Hill, R.S. (1986). Lauraceous leaves from the Eocene of Nerriga, New South Wales. *Alcheringa, 10*(4), 327–351.

Hoefs, J. (1997). *Stable isotope geochemistry (*4th ed., pp.38–43, 133–134). Berlin: Springer-Verlag.

Hofmann, A.W. & White, W.M. (1982). Mantle plumes from ancient oceanic crust. *Earth and Planetary Science Letters, 57*, 421–436.

Humphreys, D.R. (1986). Reversals of the earth's magnetic field. In R.E. Walsh, C.L. Brooks, & R.S. Crowell (Eds.), *Proceedings of the first international conference on*

*creationism (*Vol. 2, pp. 113–126). Pittsburgh, Pennsylvania: Creation Science Fellowship.

Joplin, G.A. (compiler) (1963). *Chemical analyses of Australian rocks, part 1: Igneous and metamorphic* (Bulletin 65, pp. 216–217). Canberra, Australia: Bureau of Mineral Resources, Geology and Geophysics.

Krueger, H. (1996). Letter dated May 29, 1996 to Dr. Andrew A. Snelling. (Hal Kruger is Head Laboratory Manager at Geochron Laboratories, Cambridge, Boston, USA).

Lawson, E.M. (1996). Letter dated June 28, 1996 to Dr. Andrew A. Snelling. (Dr. Ewan Lawson is a research scientist on the staff of the Antares Mass Spectrometry Laboratory, ANSTO, Lucas Heights near Sydney, Australia.)

Le Maitre, R.W., Bateman, P., Dudek, A., Keller, J., Lameyne Le Bas, M.J., Sabine, P.A., Schmid, R., Sorensen, H., Streckeisen, A., Woolley, A.R., & Zanettin, B. (1989). *A classification of igneous rocks and glossary terms.* Oxford, England: Blackwell.

Mallett, C.W., Pattison, C., McLennan, T., Balfe, P., & Sullivan, D. (1995). Bowen Basin. In C.R. Ward, H.J. Harrington, C.W. Mallett, & J.W. Beetson (Eds.), *Geology of Australian coal basins (*pp. 299–339). Geological Society of Australia Coal Geology Group, Special Publication No. 1.

Middlemost, E.A.K. (1985). Miocene shield volcanoes of New South Wales. In F.L. Sutherland, B.J. Franklin, & A.E. Waltho (Eds.), *Volcanism in eastern Australia (with case histories from New South Wales) (*pp. 49–58). Geological Society of Australia, New South Wales Division Publication No. 1.

Olgers, F. (1984). *Emerald, Queensland, 1:250,000 geological series explanatory notes.* Canberra: Bureau of Mineral Resources, Geology and Geophysics.

Park, W.J. (1975). German Creek-Emerald district. In D.M. Traves & D. King (Eds.), *Economic geology of Australia and Papua New Guinea, 2, coal (*pp. 89–92). Australasian Institute of Mining and Metallurgy, Melbourne, Monograph 6.

Patterson, C.C. (1956). Age of meteorites and the earth. *Geochimica et Cosmochimica Acta, 10*, 230–237.

Pearce, J.A. (1983). Role of the sub-continental lithosphere in magma genesis at active continental margins. In C.J. Hawkesworth & M.J. Norry (Eds.), *Continental basalts and mantle xenoliths (*pp. 230–249). Nantwich: Shiva.

Pearce, J.A. (1996). A user's guide to basalt discrimination diagrams. In D.A. Wyman (Ed.), *Trace element geochemistry of volcanic rocks: Applications for massive sulphide exploration (*Vol. 12, pp. 79–113). Geological Association of Canada, Short Course Notes.

Polach, H. & Robertson, S. (1983). *Data reduction and age calculations at the ANU radiocarbon dating research laboratory.* The Australian National University, Canberra: ANU Radiocarbon Laboratory Publication LM7.

Reesman, R. (1997). Letter dated March 17, 1997 to Dr. Andrew A. Snelling. (Dr. Richard Reesman is the K-Ar Laboratory Manager at Geochron Laboratories, Cambridge, Boston, USA).

Rollinson, H. (1993). *Using geochemical data: Evaluation, presentation, interpretation (*pp. 133–150). Harlow, England: Longman.

Rosholt, J.N. & Bartel, A.J. (1969). Uranium, thorium and lead systematics in the Granite Mountains, Wyoming. *Earth and Planetary Science Letters, 7*, 14–17.

Saunders, A.D. & Tarney, J. (1984). Geochemical characteristics of the basaltic volcanism within back-arc basins. In B.P. Kokelaar & M.F. Howells (Eds.), *Marginal basin geology (*pp. 59–76). Geological Society of London, Special Publication 16.

Snelling, A.A. (1991). The formation and cooling of dykes. *Creation Ex Nihilo Technical Journal, 5*(1), 81–90.

Snelling, A.A. (1998). The cause of anomalous potassium-argon "ages" for recent andesite flows at Mt. Ngauruhoe, New Zealand, and the implications for potassium-argon "dating." In R.E. Walsh (Ed.), *Proceedings of the fourth international conference on creationism* (pp. 503–525). Pittsburgh, Pennsylvania: Creation Science Fellowship.

Staines, H.R.E. & Koppe, W.H. (1980). The geology of the north Bowen Basin. In R.A. Henderson & P.J. Stephenson (Eds.), *The geology and geophysics of northeastern Australia (*pp. 279–298). Brisbane: Geological Society of Australia, Queensland Division.

Sun, S.S., Tatsumoto, M., & Schilling, J.-G. (1975). Mantle plume mixing along the Reykjanes Ridge axis: Lead isotopic evidence. *Science, 190*, 143–147.

Sun, S.S. (1980). Lead isotopic study of young volcanic rocks from mid-ocean ridges, ocean islands and island arcs. *Philosophical Transactions of the Royal Society of London, A297*, 409–445.

Sun, S.S. & McDonough, W.F. (1989). Chemical and isotopic systematics of oceanic basalts: Implications for mantle composition and processes. In A.D. Saunders & M.J. Norry (Eds.), *Magmatism in ocean basins* (pp. 313–345). Geological Society of London, Special Publication 42.

Sutherland, F.L. (1978). Mesozoic-Cainozoic volcanism of Australia. In E. Scheibner (Ed.), The Phanerozoic structure of Australia and variations in tectonic style. *Tectonophysics, 48*, 413–427.

Sutherland, F.L. (1985). Regional controls in eastern Australian volcanism. In F.L. Sutherland, B.J. Franklin, & A.E. Waltho (Eds.), *Volcanism in eastern Australia (with case histories from New South Wales)* (pp. 13–32). Geological Society of Australia, New South Wales Division Publication No. 1.

Weaver, B. & Tarney, J. (1984). Empirical approach to estimating the composition of the continental crust. *Nature, 310*, 575–577.

Webb, A.W. & McDougall, I. (1967). A comparison of mineral and whole rock potassium-argon ages of Tertiary volcanics from Central Queensland, Australia. *Earth and Planetary Science Letters, 3*, 41–47.

Webb, A.W. (1995). *K-Ar Dating of two volcanic rocks.* Amdel Limited Mineral Services Laboratory, Report G87830OG/95.

Wilcox, G. (1996). Letter dated February 1, 1996 to Dr. Andrew A. Snelling. (Gwen Wilcox is a laboratory manager at Geochron Laboratories, Cambridge, Boston, USA).

Winchester, J.A. & Floyd, P.A. (1977). Geochemical discrimination of different magma series and their differentiation products using immobile elements. *Chemical Geology, 20*, 325–343.

Woodhead, J.D., Volker, F., & McCulloch, M.T. (1995). Routine lead isotope determinations using a lead-207-lead-204 double spike: A long-term assessment of analytical precision and accuracy. *Analyst, 120*, 35–39.

Wellman, P. (1983). Hotspot volcanism in Australia and New Zealand: Cainozoic and mid-Mesozoic. *Tectonophysics, 96*(3-4), 225–243.